Credits: Geoff Chen

Towards cosmological parameters with SPT-3G TTTEEE - 19/20 CMB data

Etienne Camphuis (Institut d'Astrophysique de Paris)

Wei Quan (University of Chicago)

with Silvia Galli, Karim Benabed and Eric Hivon (IAP)

with SPT-3G collaboration

mm-Universe conference - Wednesday , June 28th 2023

South Pole Telescope and SPT-3G instrument

SPT by A. Choshki

Sobrin et al. 2022

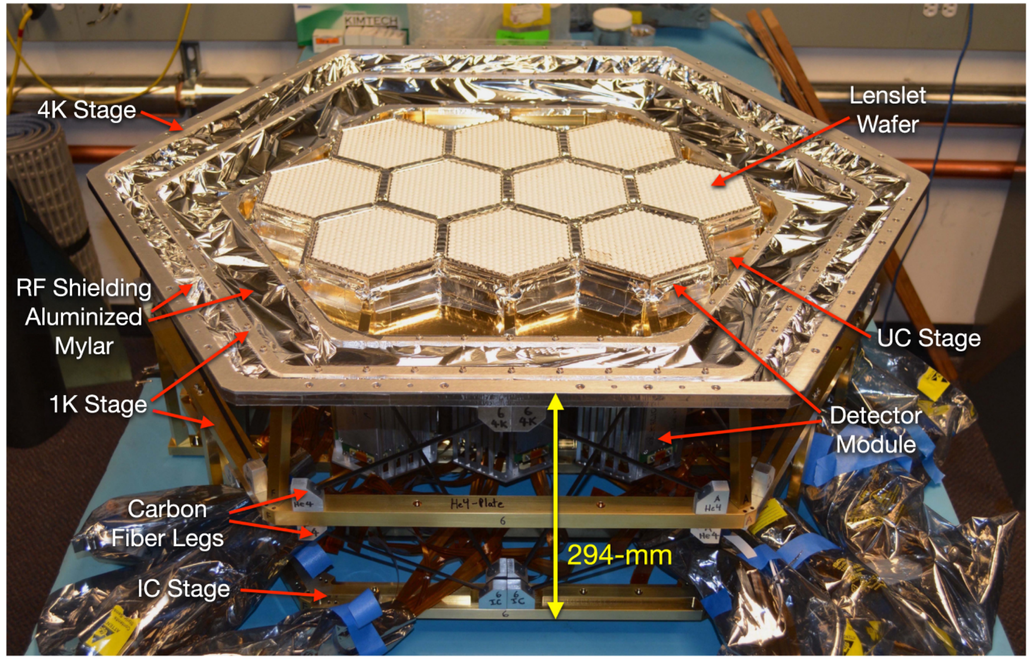

10-meter diameter telescope located at the South Pole in optimal conditions for millimeter wavelength observations

- SPT-3G: state-of-the art instrument with 3 frequencies 95, 150, 220 GHz
- Beam: 1.6'/1.2'/1.0' (*Planck*: 9.7/7.2/5.0') **High resolution**
- **~16k detectors: low noise-levels**

Science goals

- **Cosmological constraints from CMB primary anisotropies**
- **Clusters**
- **DES x SPT**
- **tSZ kSZ**
- CMB lensing
- Delensing in the BICEP/Keck field
- High-l TT
- Low-l BB
- Spatially varying cosmic birefringence
- Axions
- Point sources, transients, asteroids, planet 9
- ...

SPT collaboration - July 2022

Cosmic Microwave Background

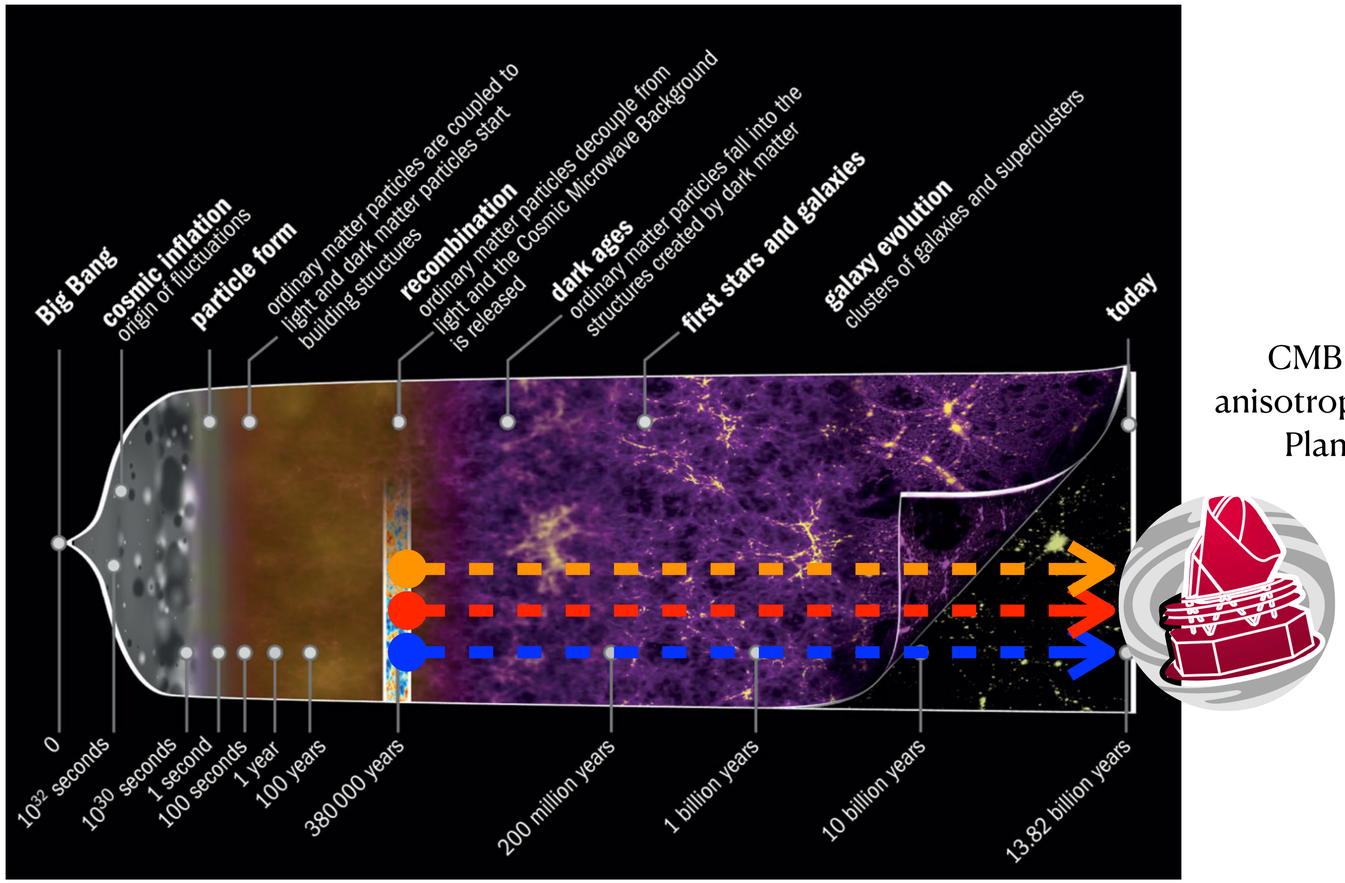

Courtesy:
ESA/C Carreau
ESA and the Planck Collaboration

CMB temperature anisotropies observed by Planck (SMICA)

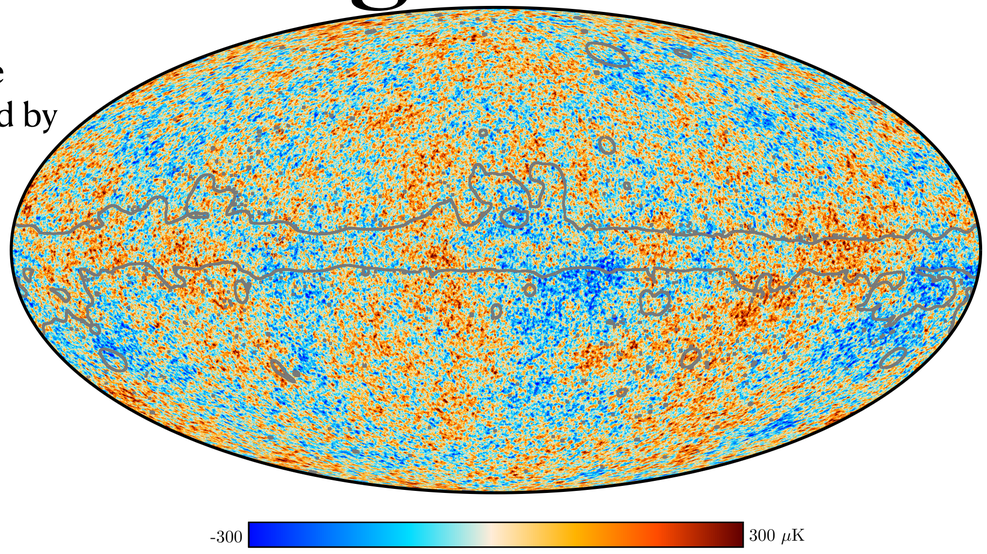

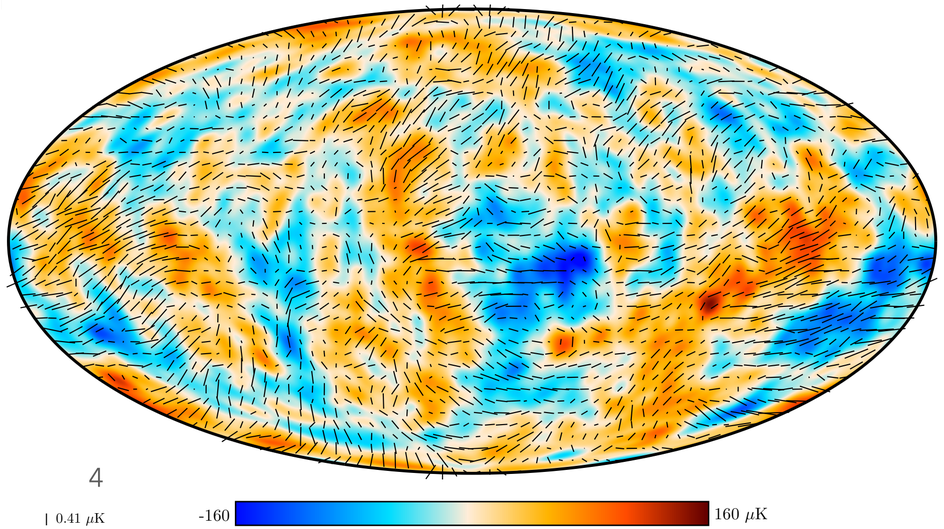

CMB polarization anisotropies

Goals of CMB science

Tensions and unkowns

Plots adapted from Balkenhol et al. 2022

H_0 tension : ~5σ

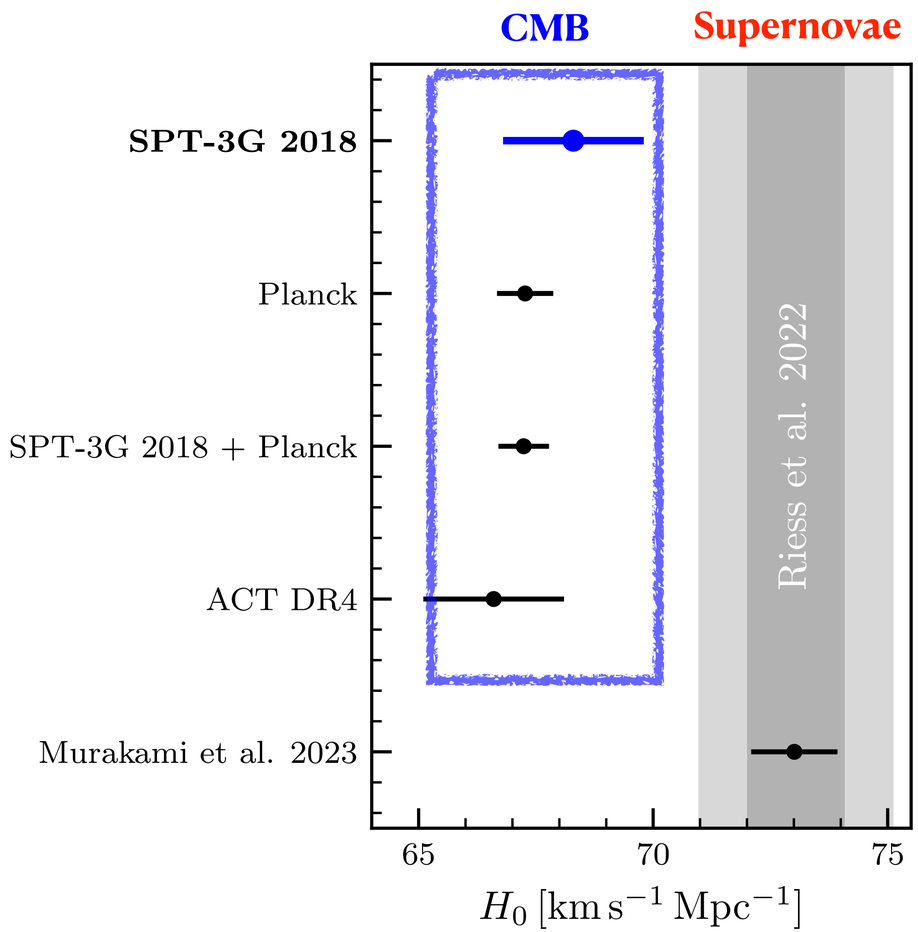

S_8 tension : ~2.5σ

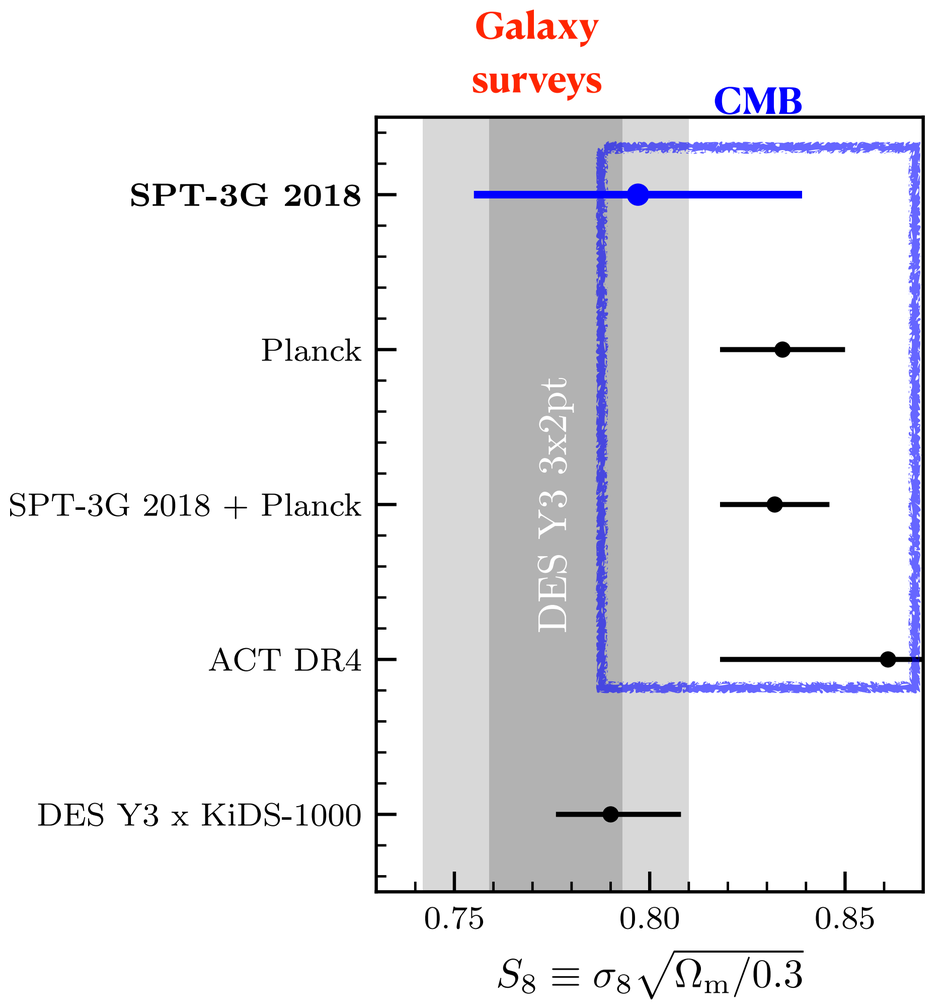

Goals of CMB science

Tensions and unkowns

Plots adapted from Balkenhol et al. 2022

H_0 tension : ~5σ

Murakami, Riess et al. 2023 - 5.7σ - 10 years of Hubble tension

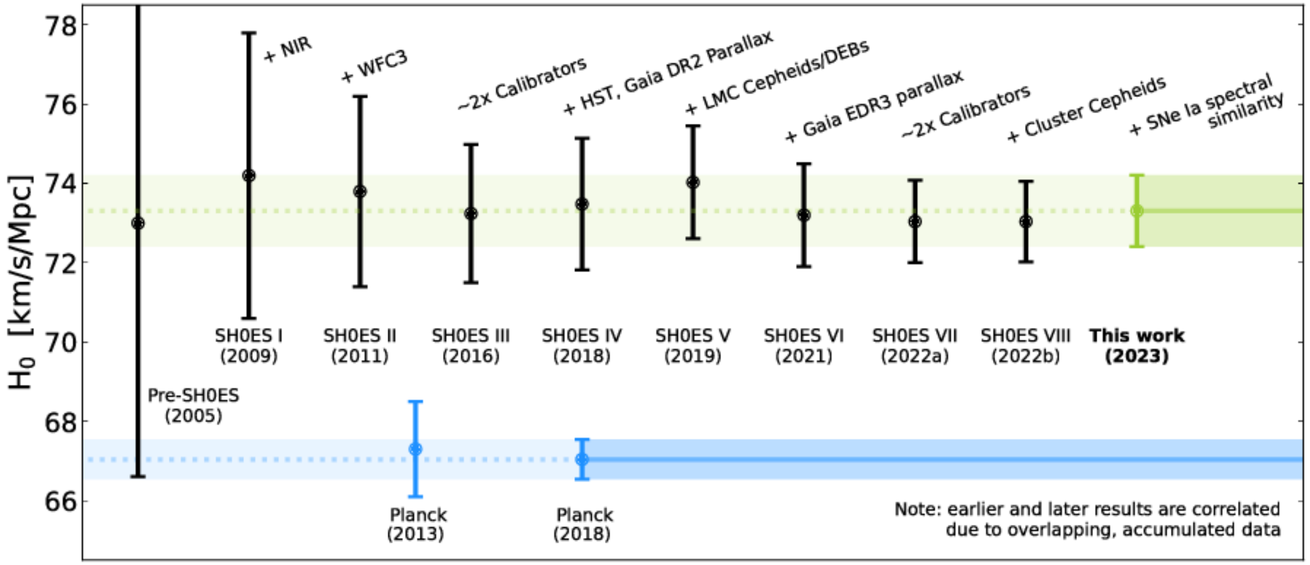

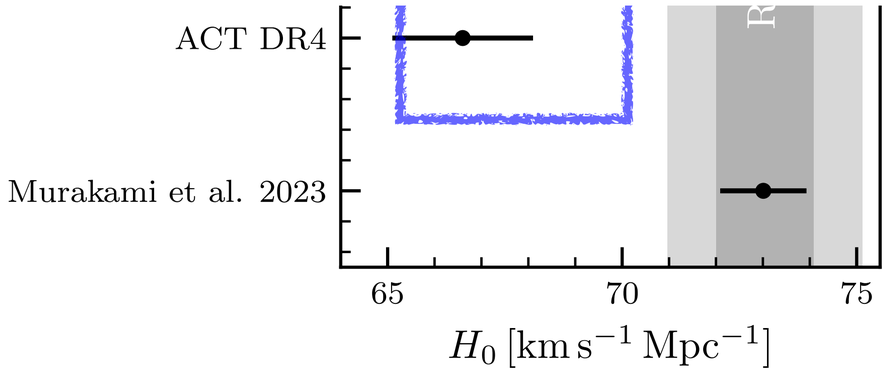

S_8 tension : ~2.5σ

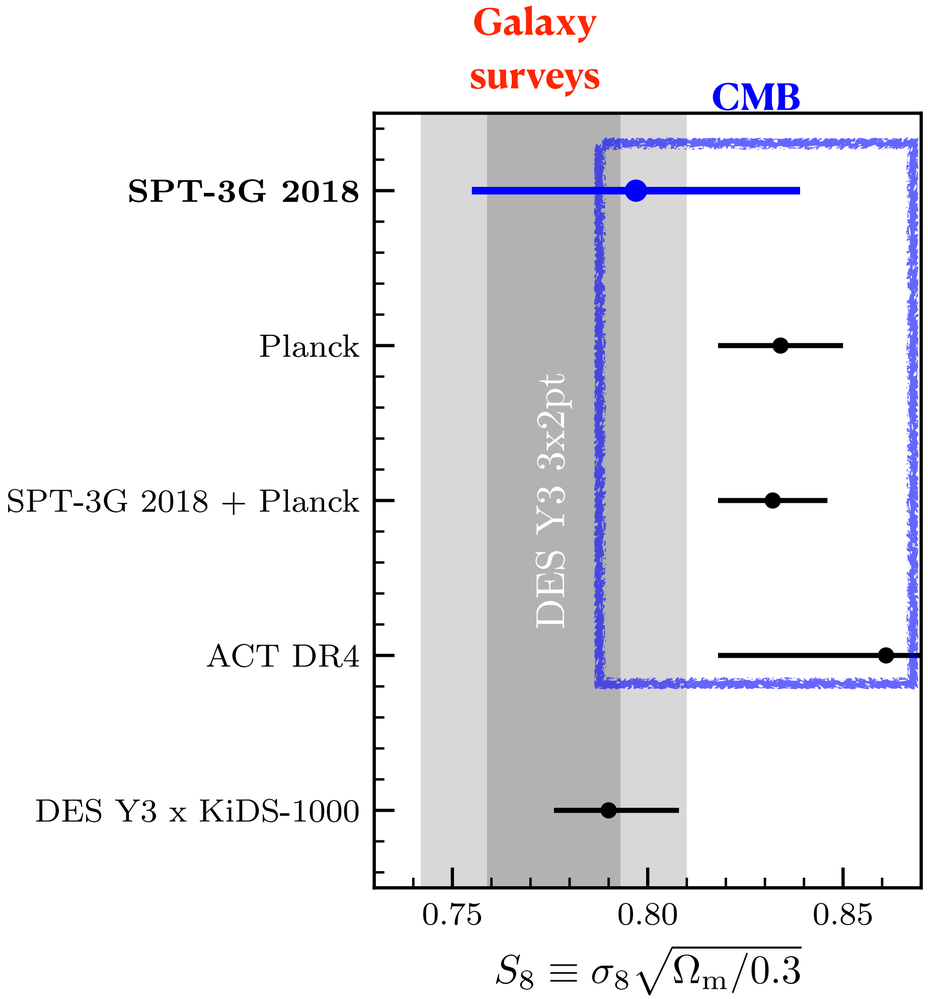

SPT-3G 2018

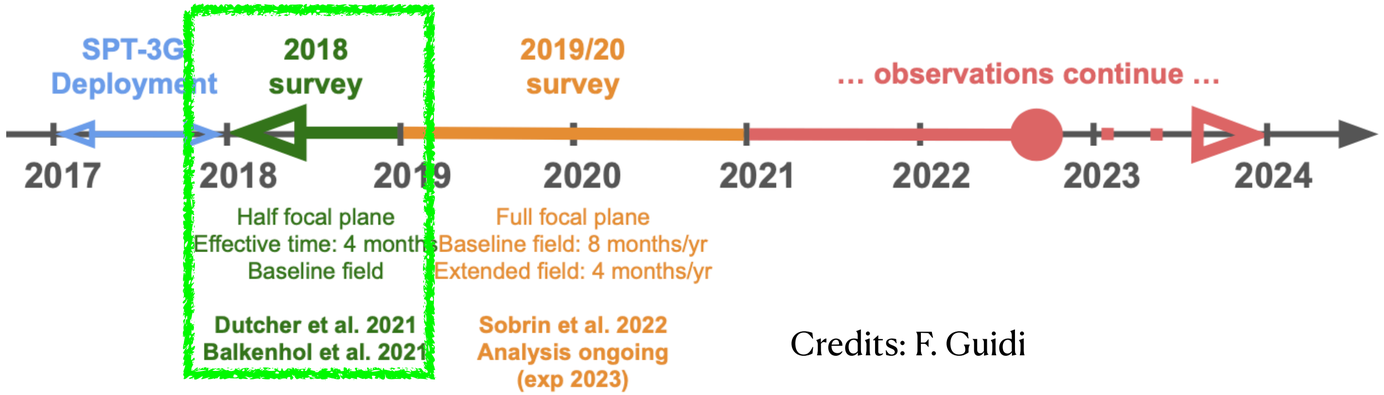

Credits: F. Guidi

SPT-3G Winter field

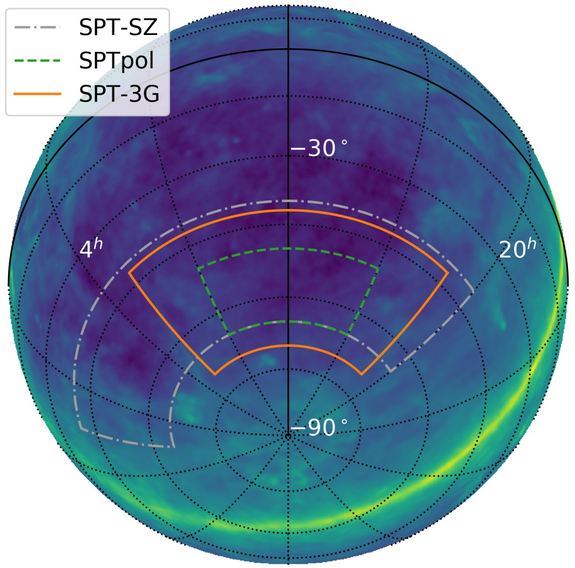

- 4% sky = 1700 sq deg
- T@150GHz noise: 15 μK-arcmin
- Lead to SPT's tightest CMB cosmological constraints with most of the SPT constraining power from EE/TE. Adding TT breaks degeneracies and improves constraints of ΛCDM by ~10–30%

SPT-3G 2018

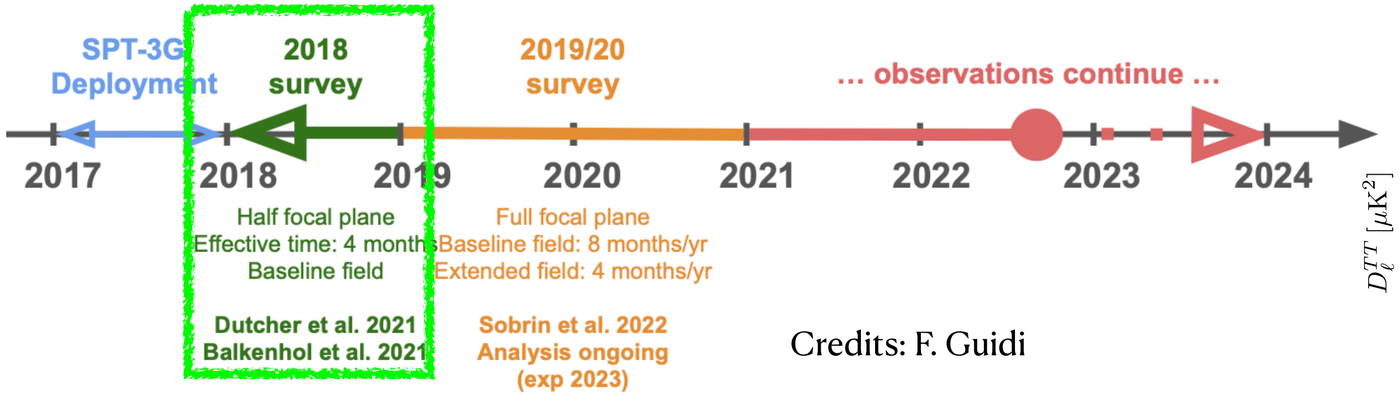

Credits: F. Guidi

SPT-3G Winter field

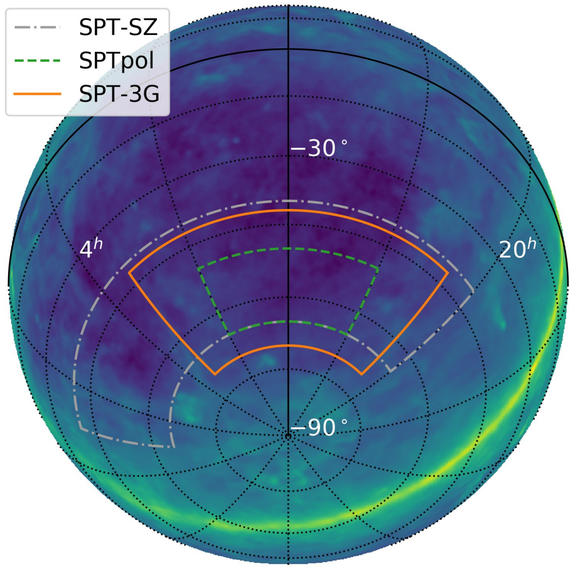

- 4% sky = 1700 sq deg
- T@150GHz noise: 15 μK-arcmin
- Lead to SPT's tightest CMB cosmological constraints with most of the SPT constraining power from EE/TE. Adding TT breaks degeneracies and improves constraints of ΛCDM by ~10–30%

CMB power spectrum measurements

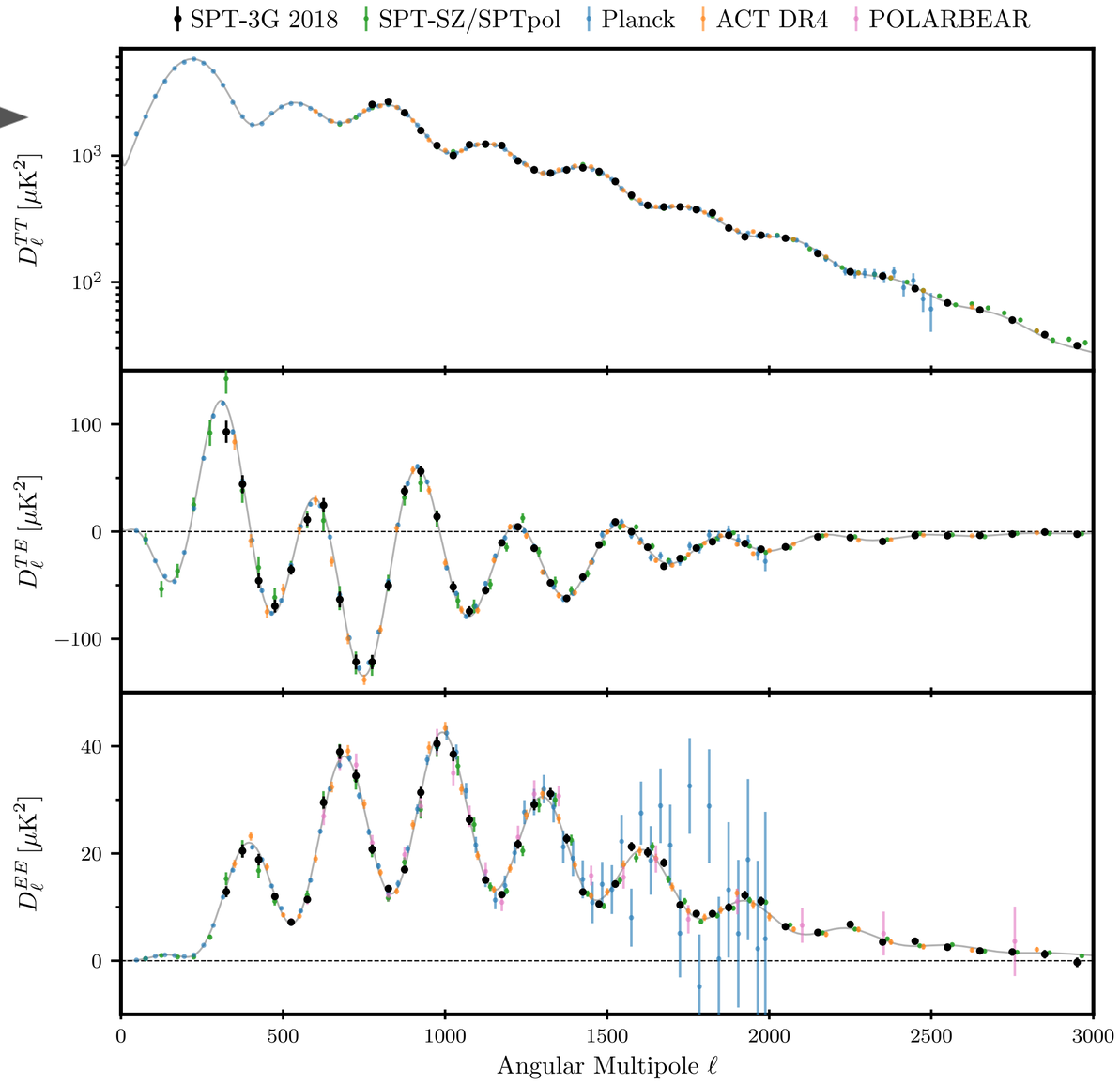

SPT-3G 2018

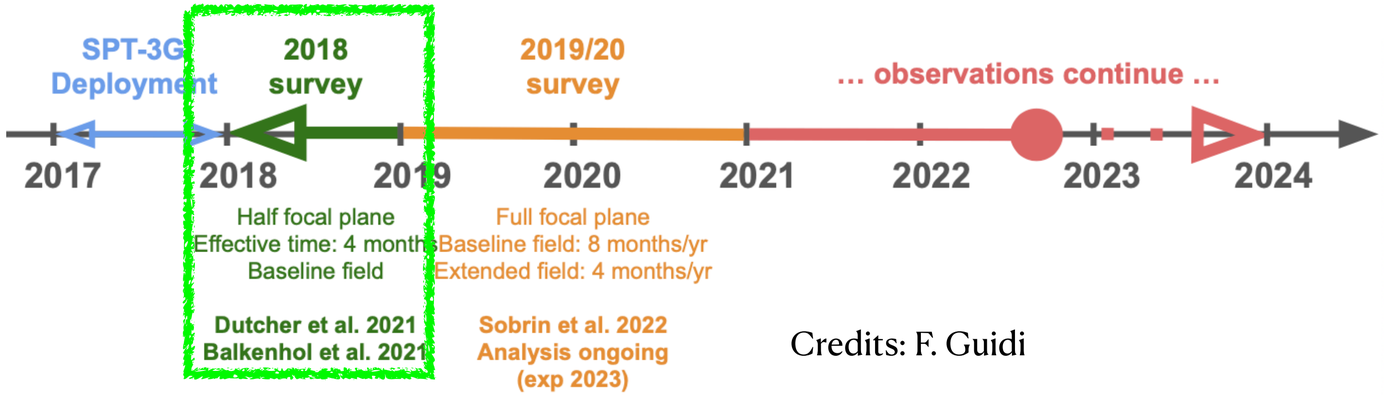

Credits: F. Guidi

SPT-3G Winter field

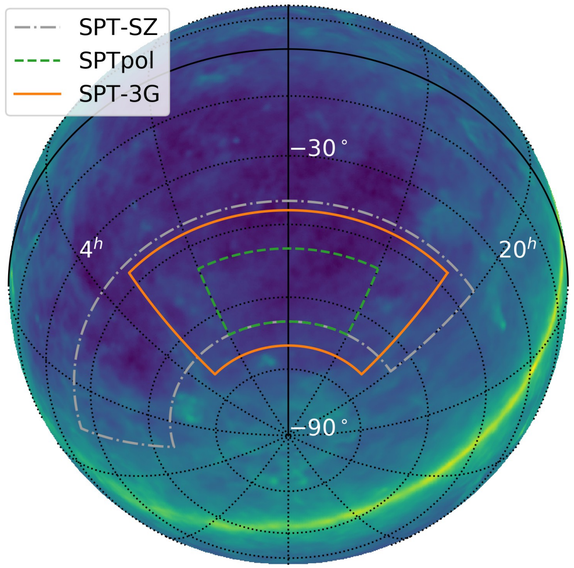

- 4% sky = 1700 sq deg
- T@150GHz noise: 15 μK-arcmin
- Lead to SPT's tightest CMB cosmological constraints with most of the SPT constraining power from EE/TE. Adding TT breaks degeneracies and improves constraints of ΛCDM by ~10–30%

ΛCDM parameters with only TE/EE [Dutcher et al. 2021]

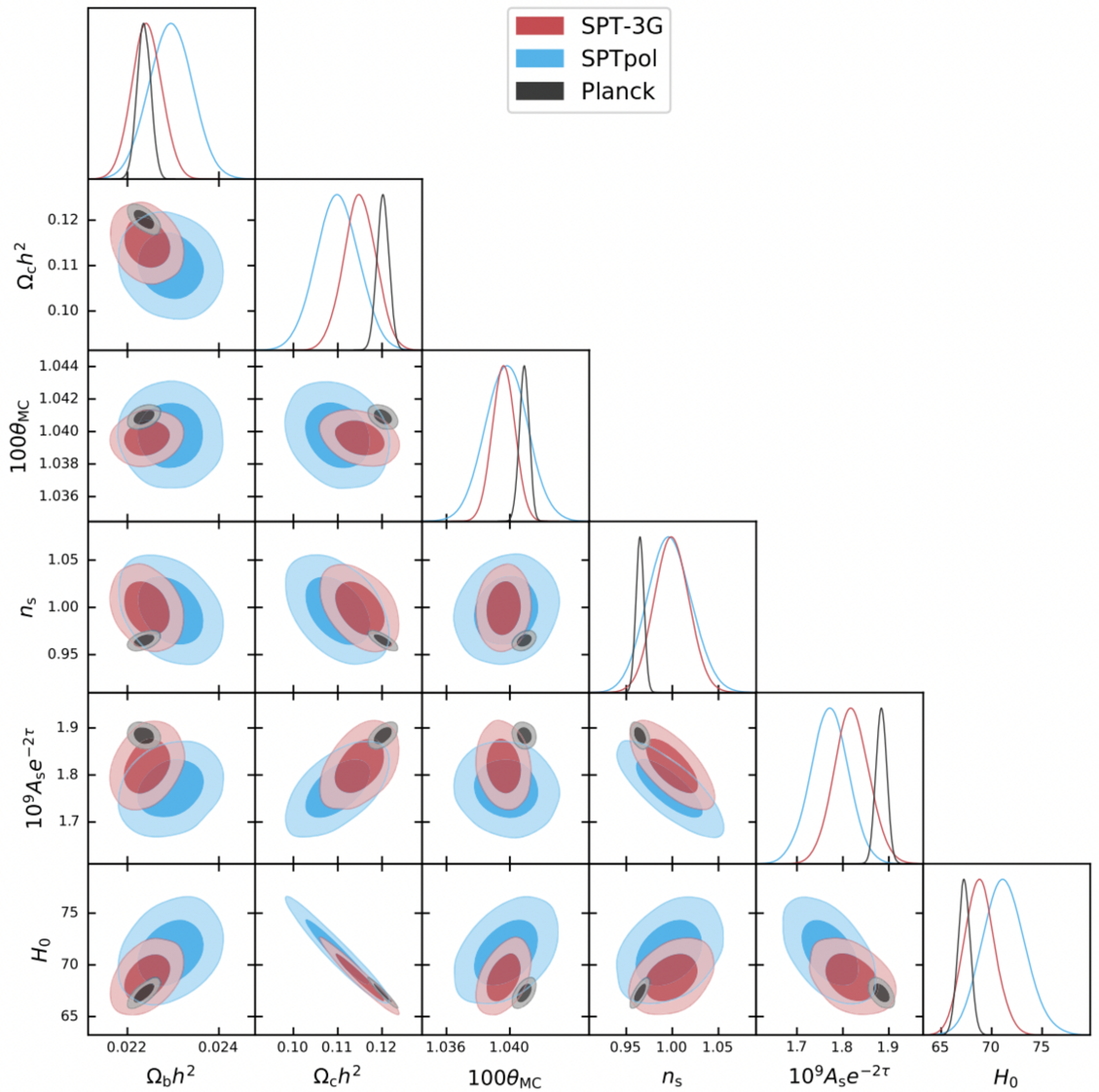

SPT-3G 2018

$H_0 = 68.3 \pm 1.5$km/s/Mpc
$S_8 = 0.797 \pm 0.042$

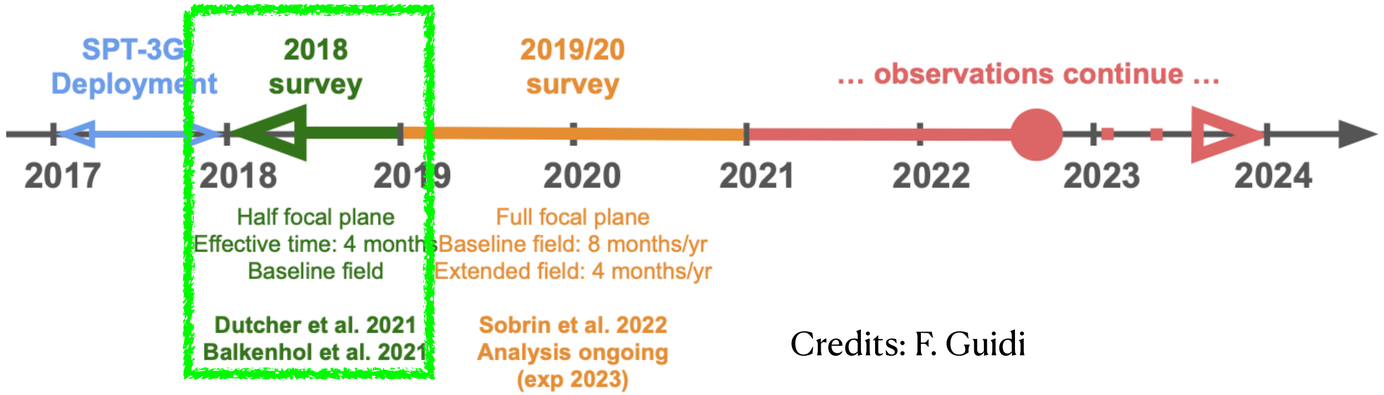

Credits: F. Guidi

SPT-3G Winter field

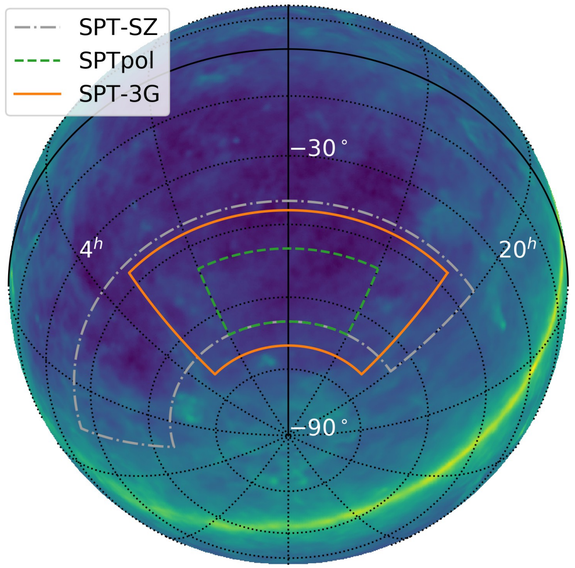

- 4% sky = 1700 sq deg
- T@150GHz noise: 15 μK-arcmin
- Lead to SPT's tightest CMB cosmological constraints with most of the SPT constraining power from EE/TE. Adding TT breaks degeneracies and improves constraints of ΛCDM by ~10–30%

ΛCDM parameters with TT/TE/EE SPT-3G 2018 - [Balkenhol et al. 2022]

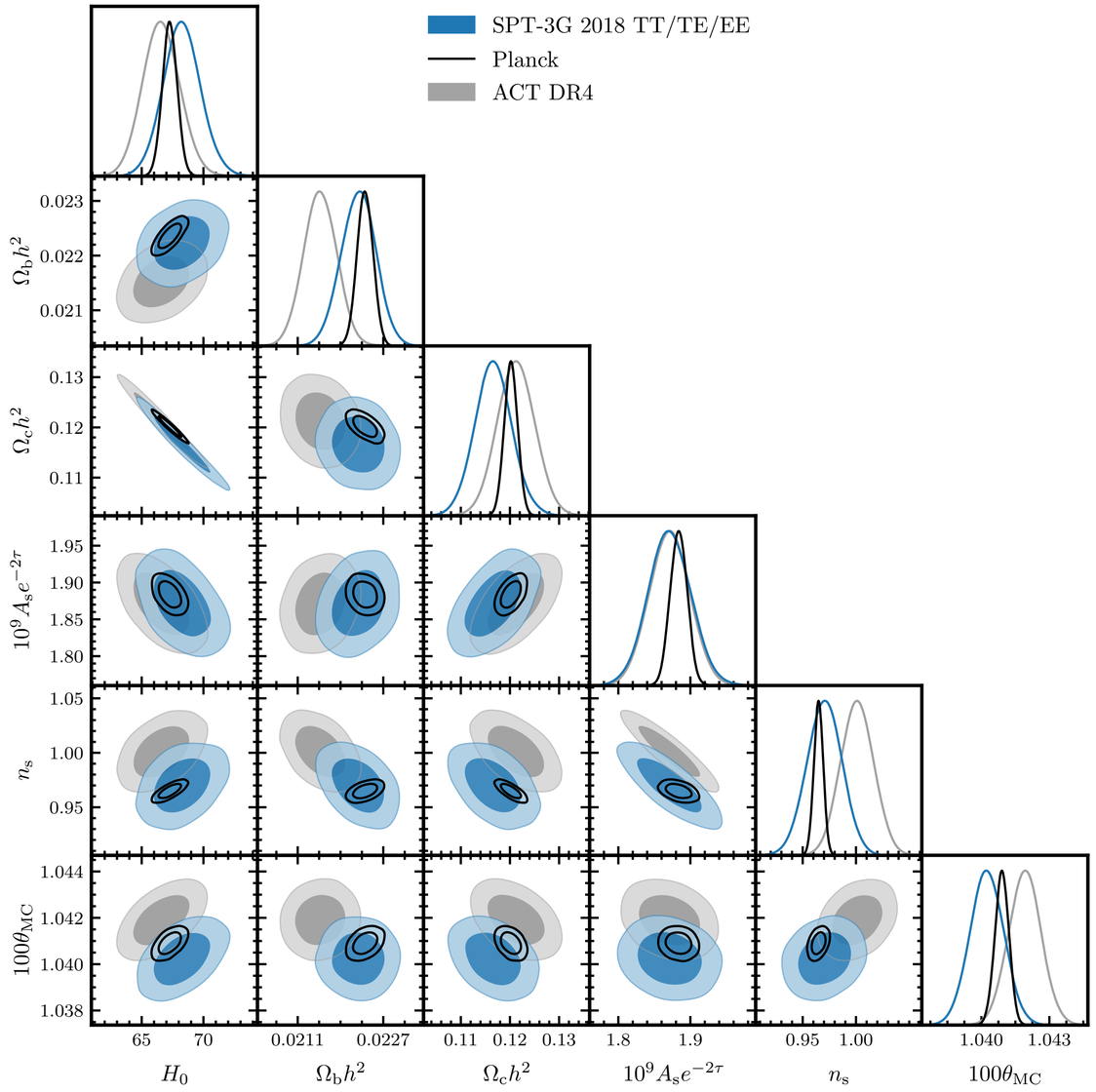

SPT-3G 2019-2023 baseline

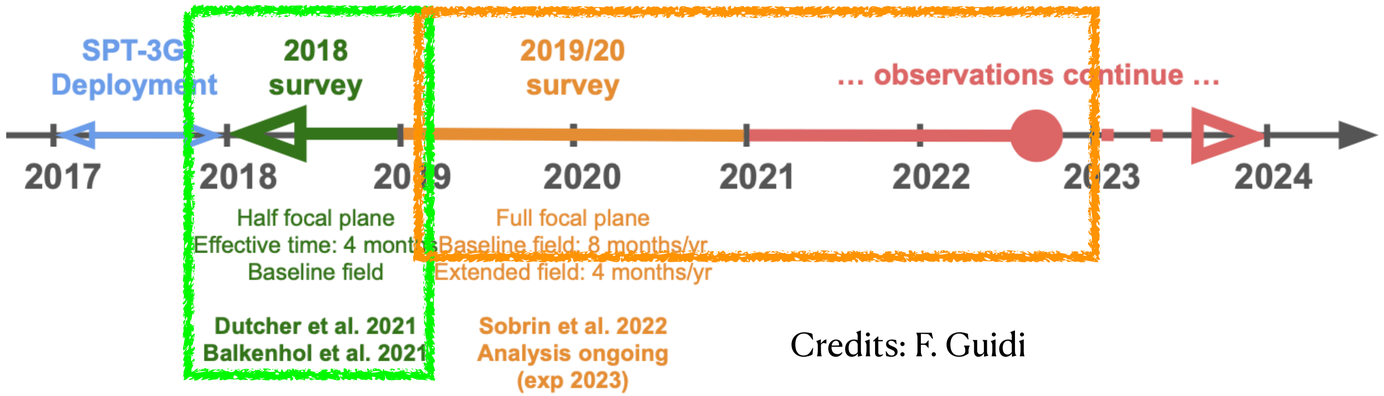

Credits: F. Guidi

SPT-3G Winter field

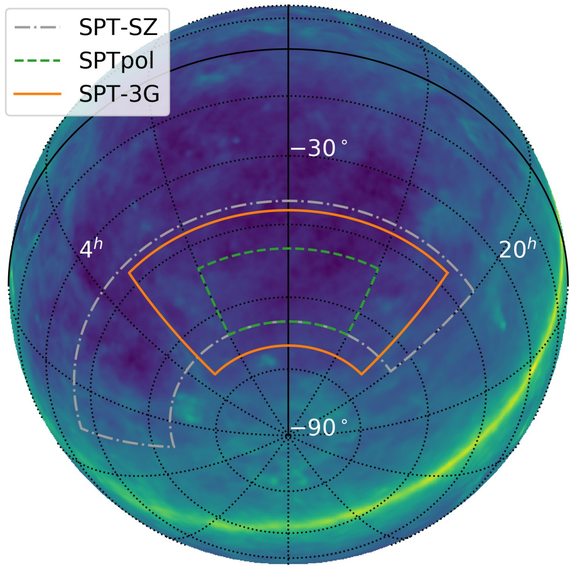

- Final noise @ T150GHz
  2.6 μK-arcmin
  Planck @ T143GHz
  40 μK-arcmin
- Final constraints on cosmological parameters comparable to Planck from independent dataset

SPT-3G 2019-2023 baseline

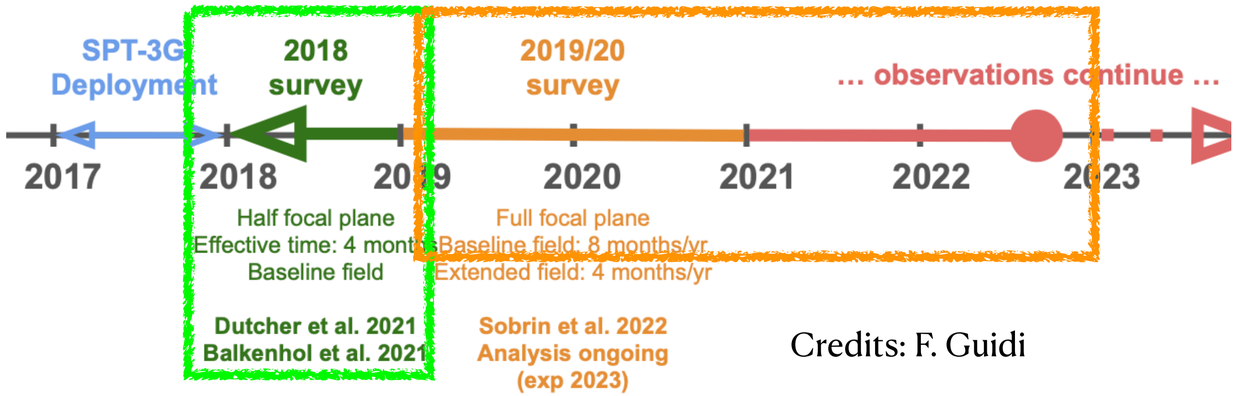

Credits: F. Guidi

SPT-3G Winter field

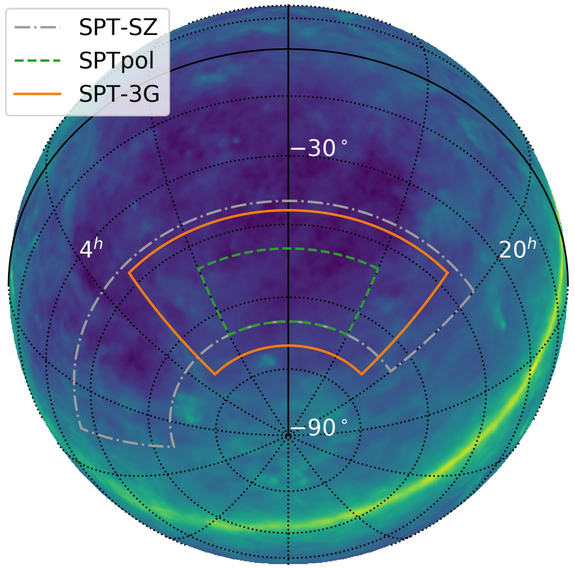

- Final noise @ T150GHz 2.6 μK-arcmin
  Planck @ T143GHz 40 μK-arcmin
- Final constraints on cosmological parameters comparable to Planck from independent dataset

SPT-3G 5YR baseline forecasts

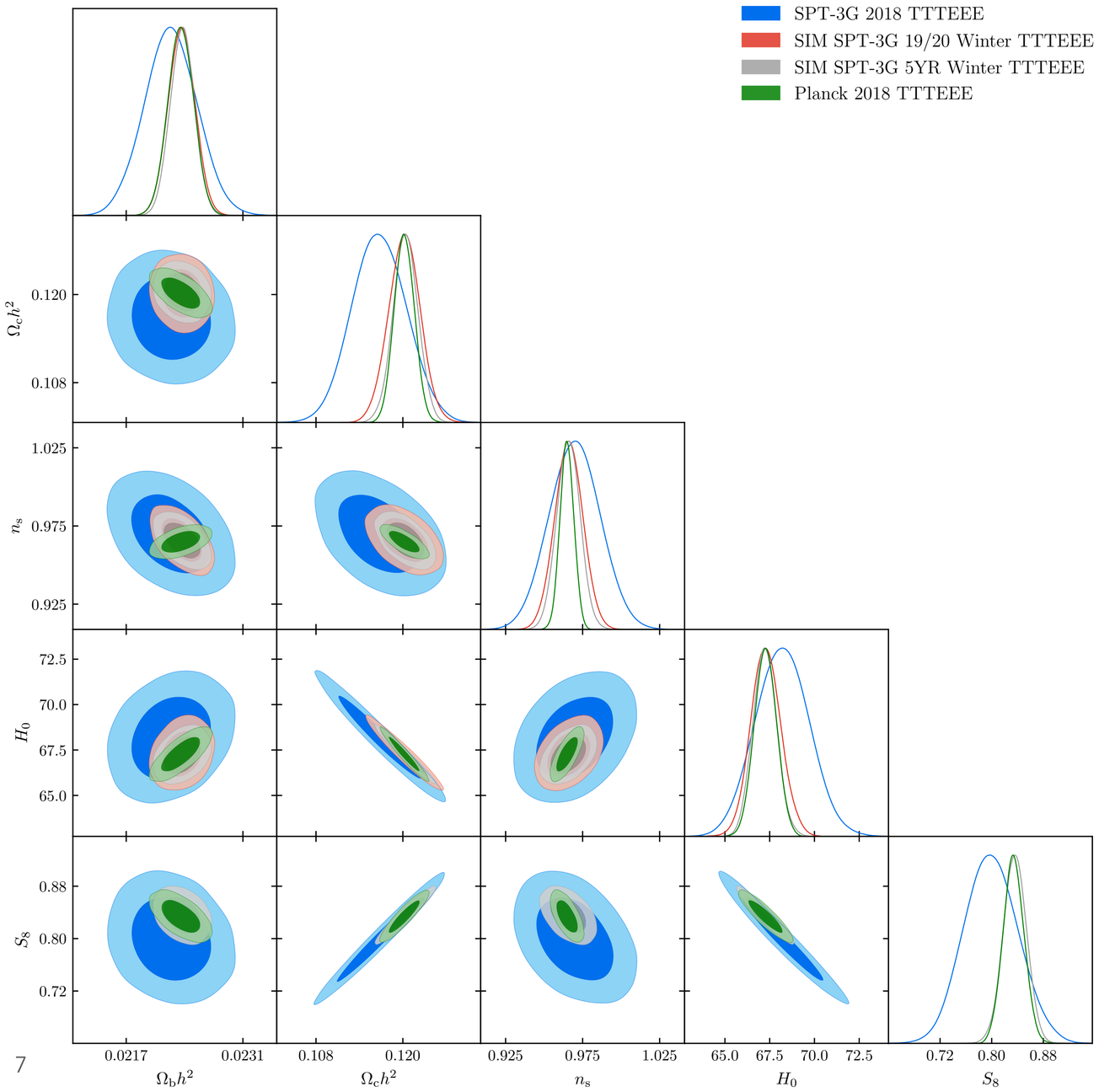

SPT-3G 2019-2020 baseline

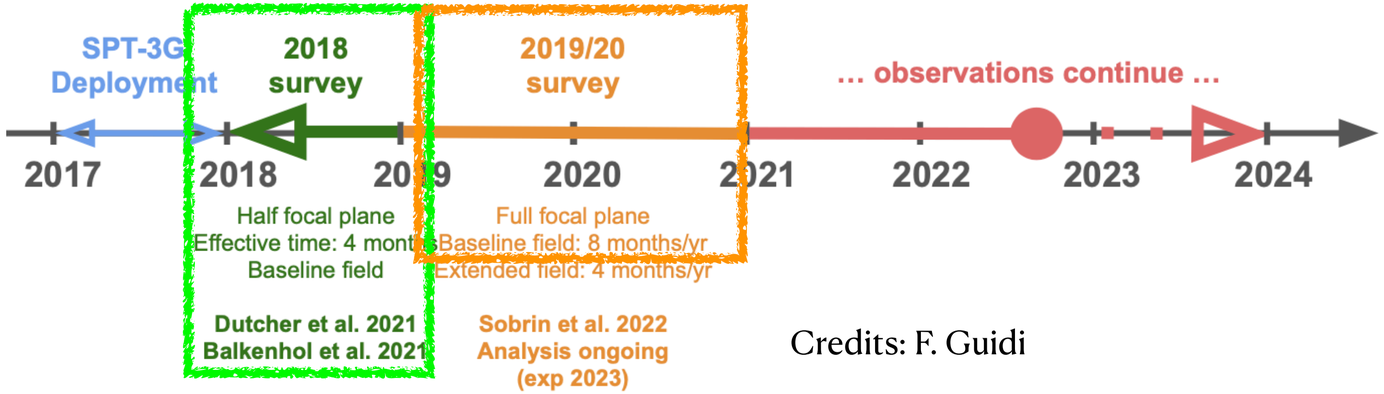

Credits: F. Guidi

SPT-3G Winter field

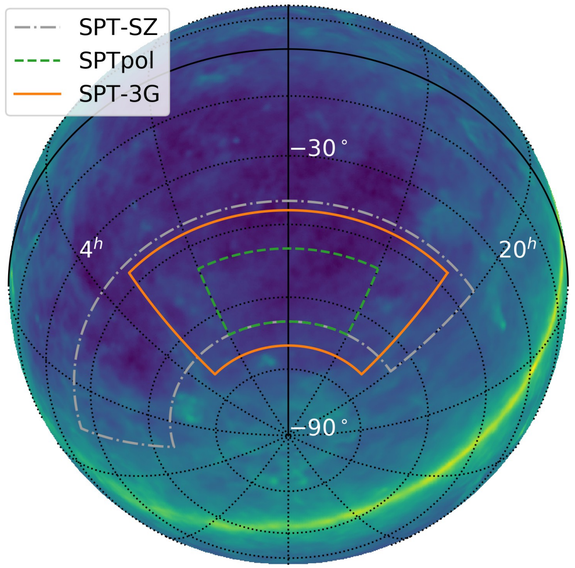

- Preliminary band powers (uncalibrated)
- Associated error bars are square root of covariance matrix

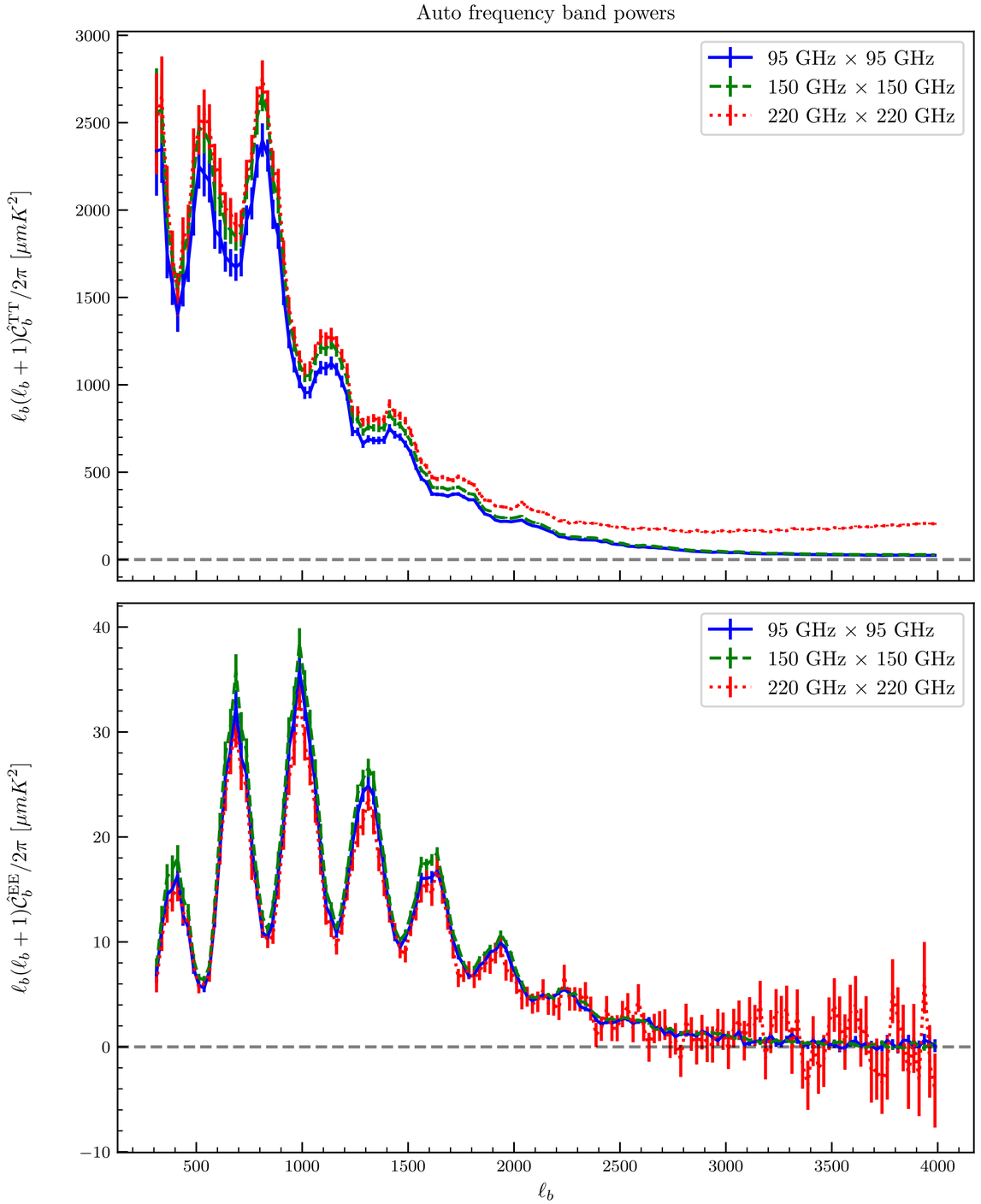

SPT-3G 2019-2020 baseline

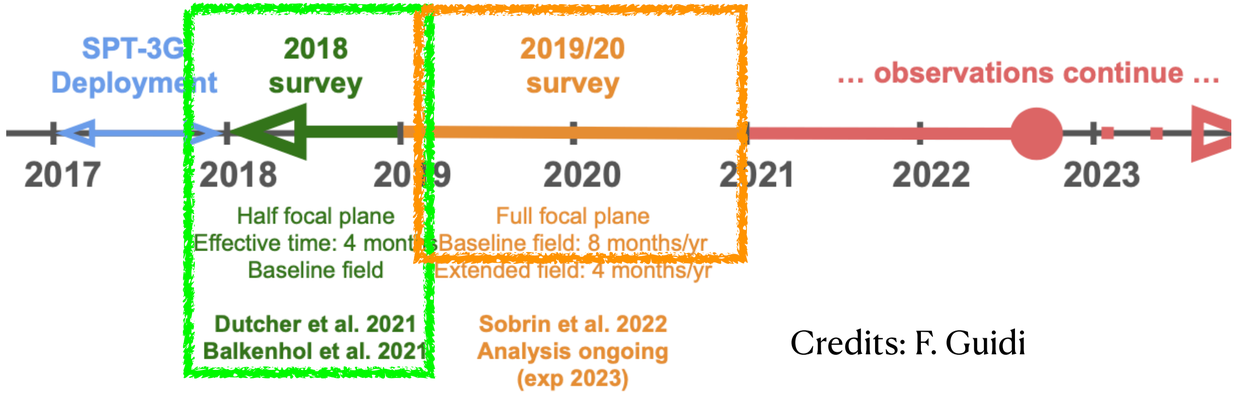

Credits: F. Guidi

SPT-3G Winter field

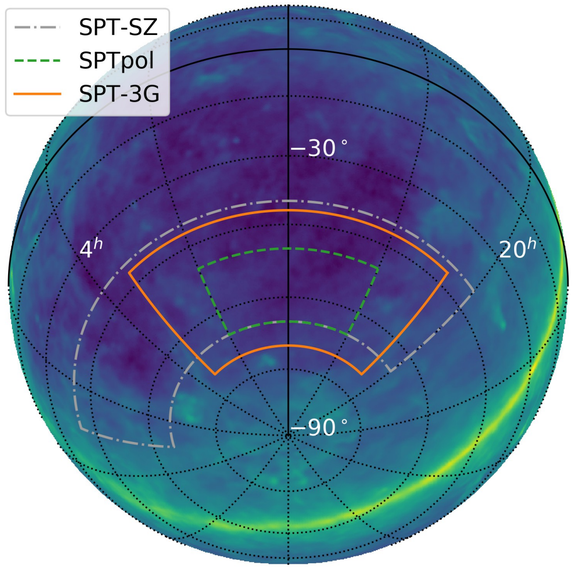

- Noise @T150GHz of 5 μK-arcmin
  3 times better than 2018
- Constraints on cosmological parameters only 10% wider than full 5 years

SPT-3G 19/20 baseline forecasts

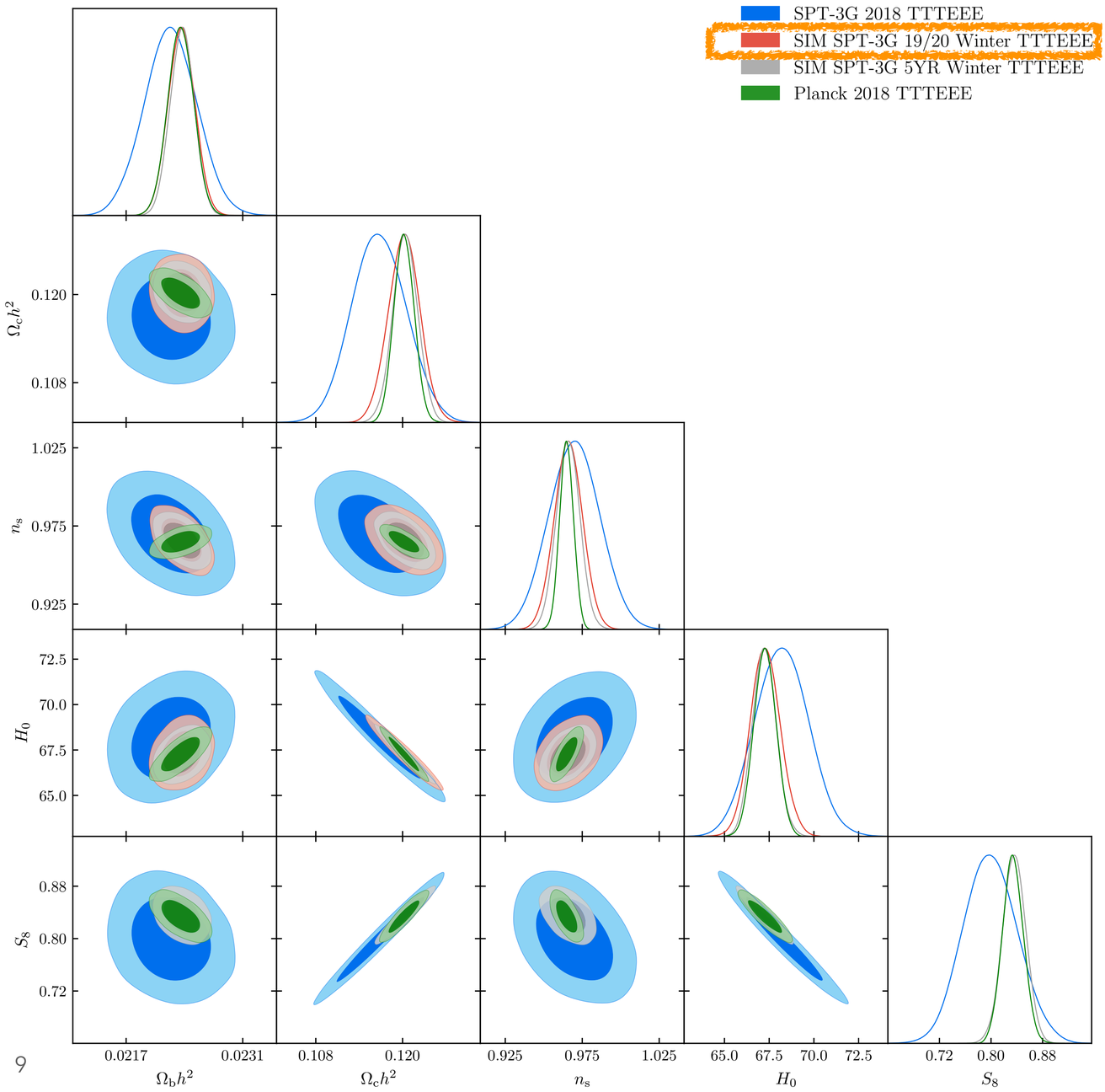

SPT-3G Extended fields

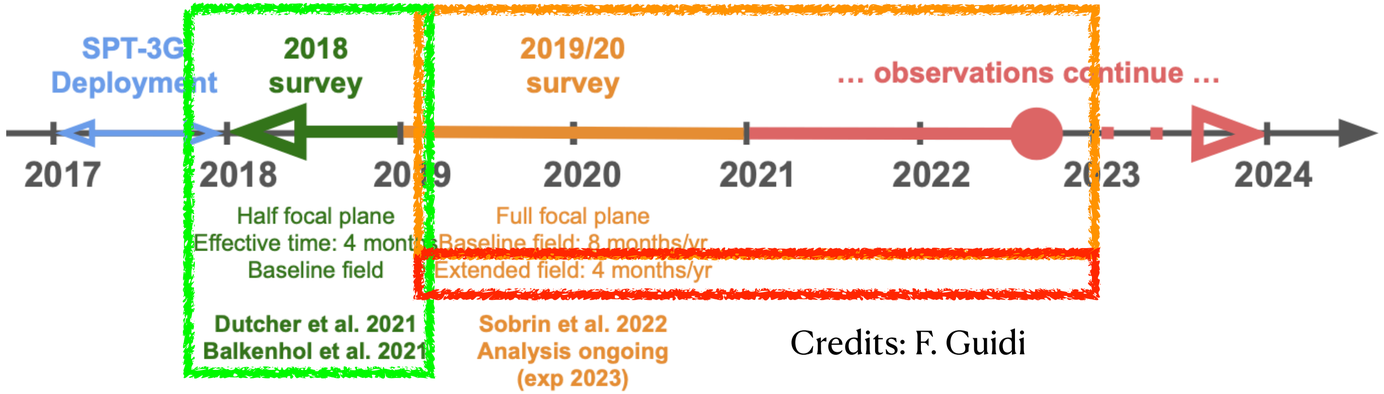

Credits: F. Guidi

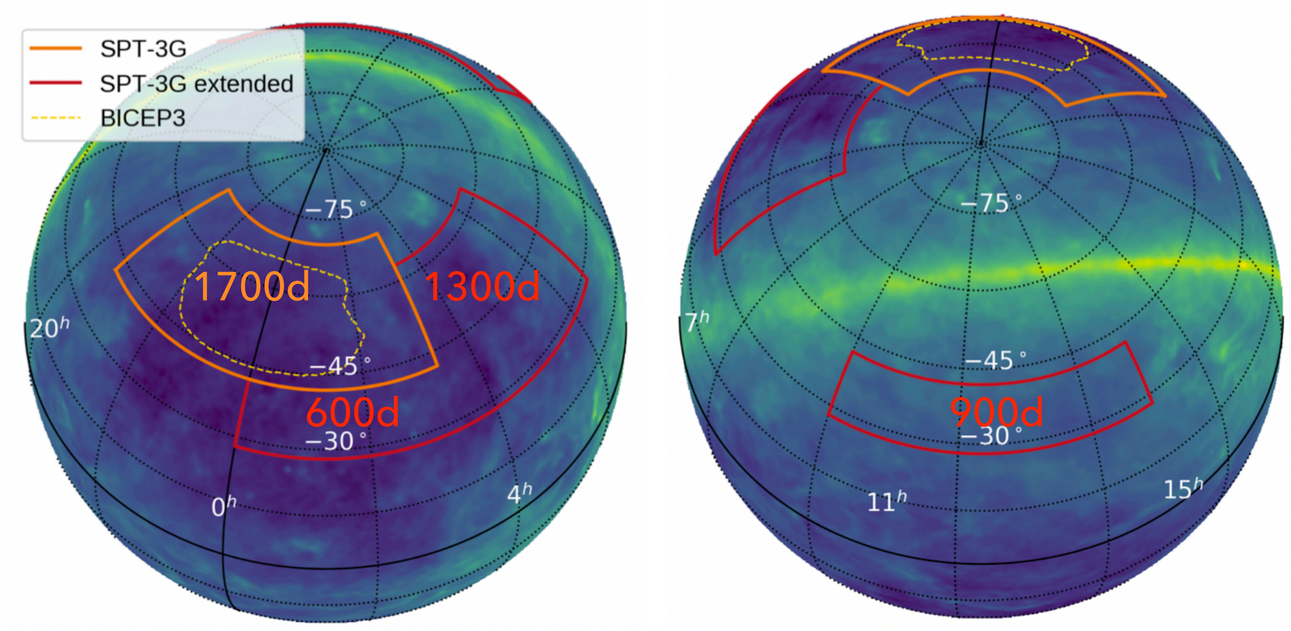

Winter field in orange, summer fields in red

- Additional sky fraction +2800 deg2
- Noise (95/150/220GHz,pol): 18.2, 17.7, 62.4 μK-arcmin

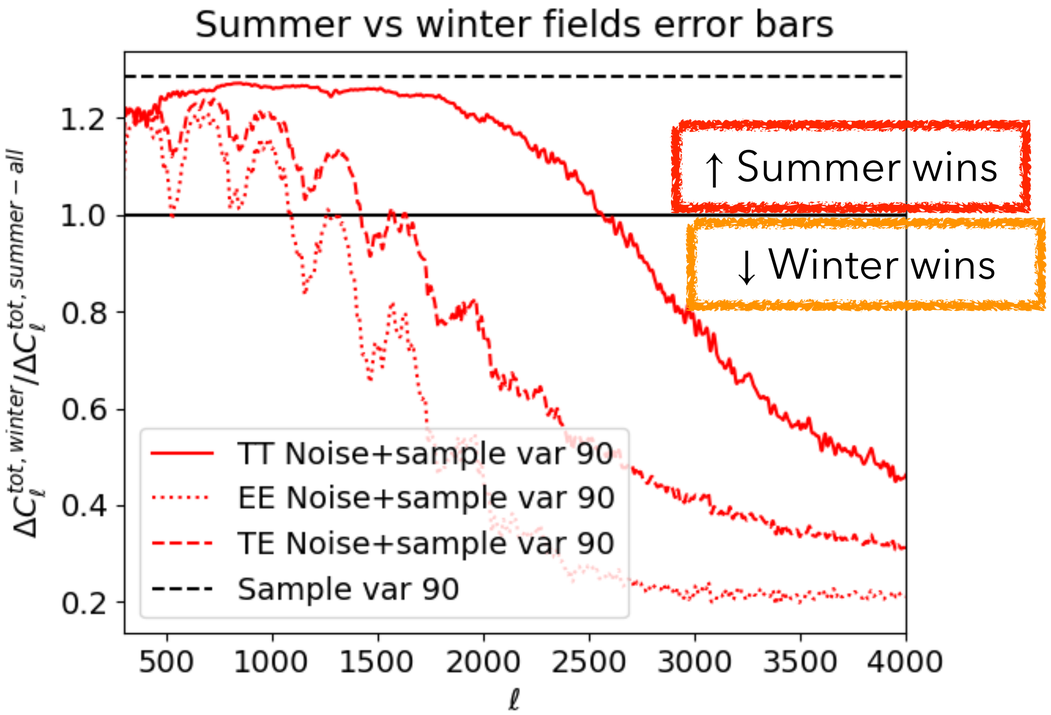

- 15 to 20 % additional constraints on final ΛCDM parameters
- Even more for ΛCDM extensions, with up to 40% for ΛCDM+$N_{\rm eff}$

SPT-3G all fields

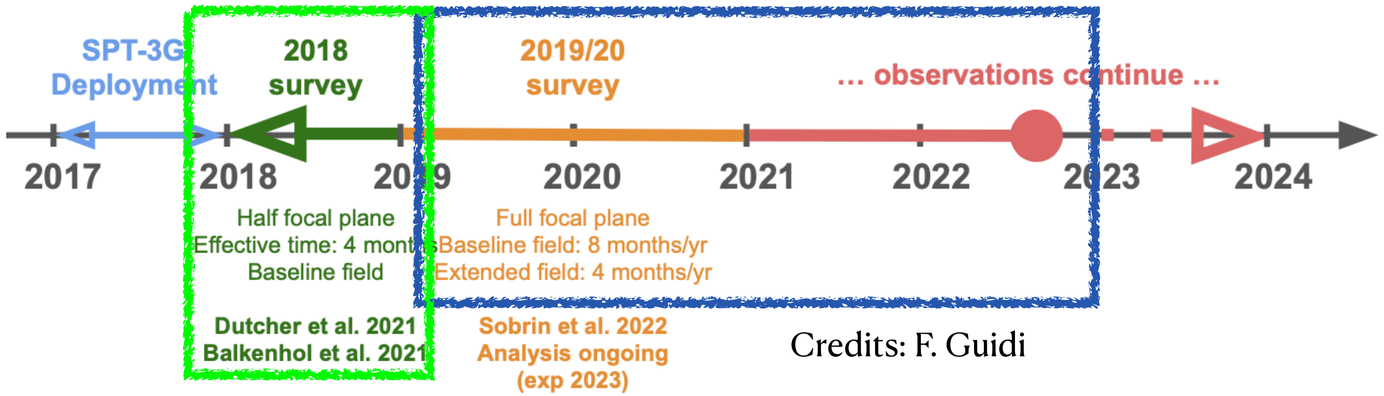

Credits: F. Guidi

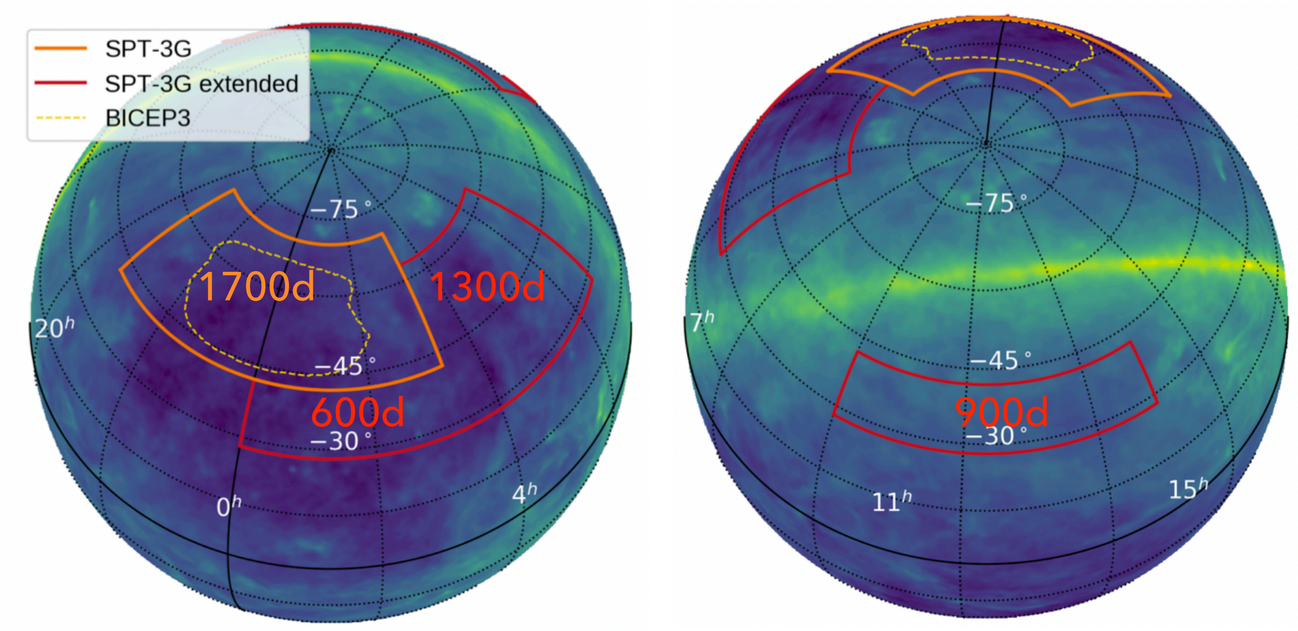

Winter field in orange, summer fields in red

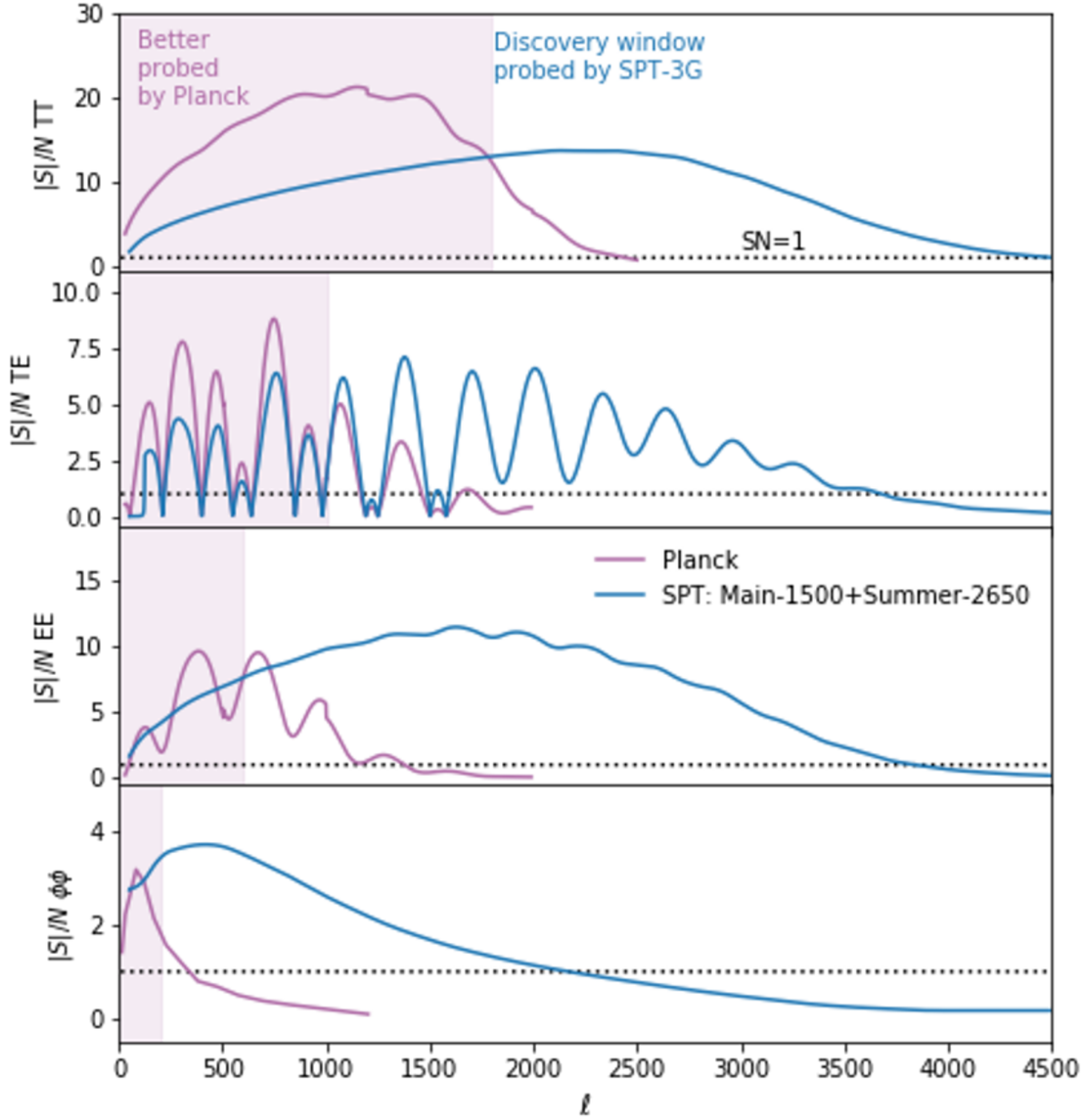

Pipeline improvements 2018 —> 2019-2020

- Flat sky —> curved sky

CMB analysis pipeline - from Hu et al. 1997

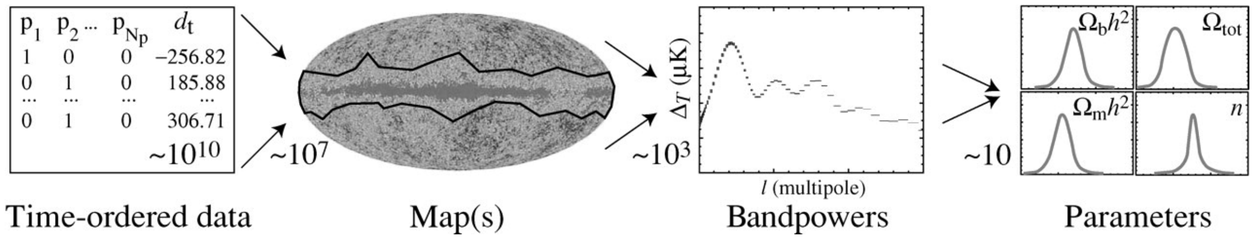

SPT-3G 2018 EE/TE covariance

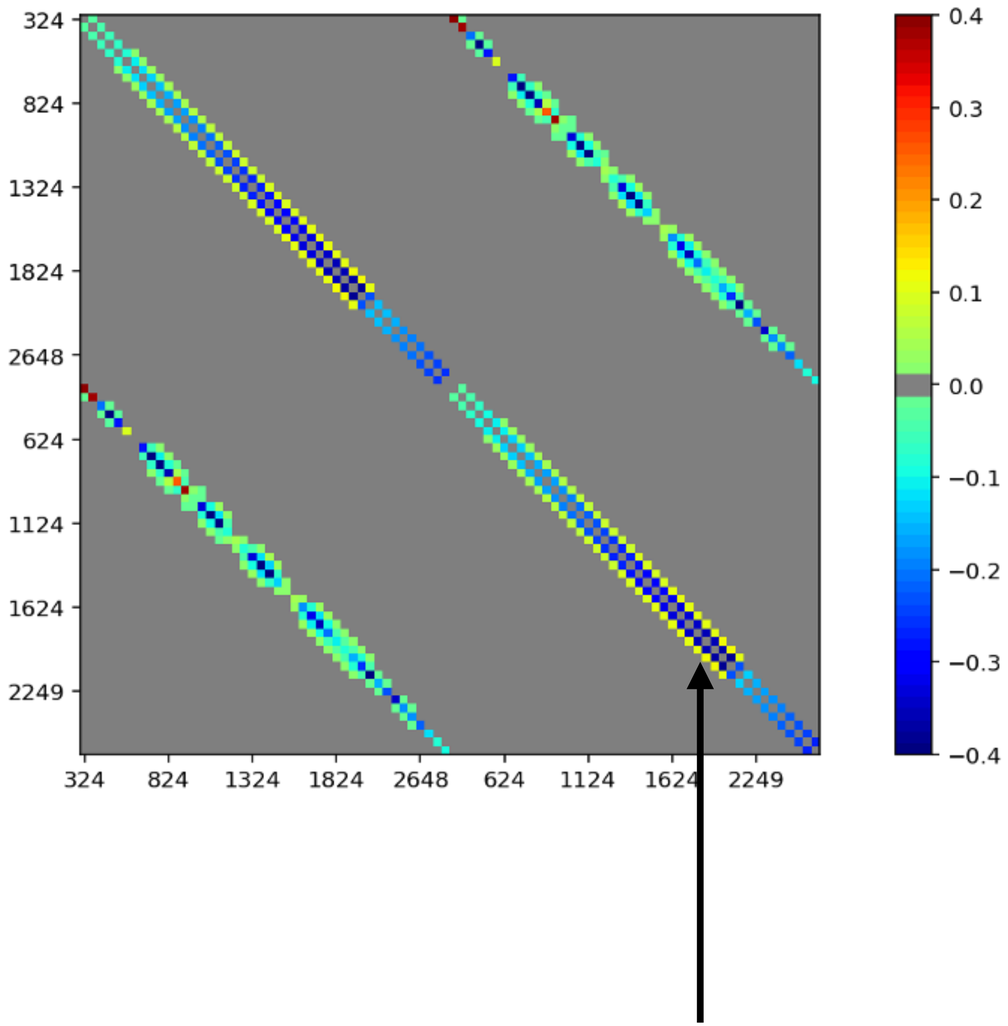

Allowed us to get rid of mode-coupling

Pipeline improvements 2018 —> 2019-2020

- Flat sky —> curved sky
- Covariance matrix from simulations —> Fast and accurate analytical computation of the covariance **[EC et al. 2022]**

Power spectrum gaussian likelihood :

$$-\ln \mathscr{L}(\hat{C} \,|\, \Lambda\mathrm{CDM})$$

$$\propto \frac{1}{2}(\hat{C} - C^{\mathrm{th}})^T \boxed{\Sigma^{-1}} (\hat{C} - C^{\mathrm{th}}))$$

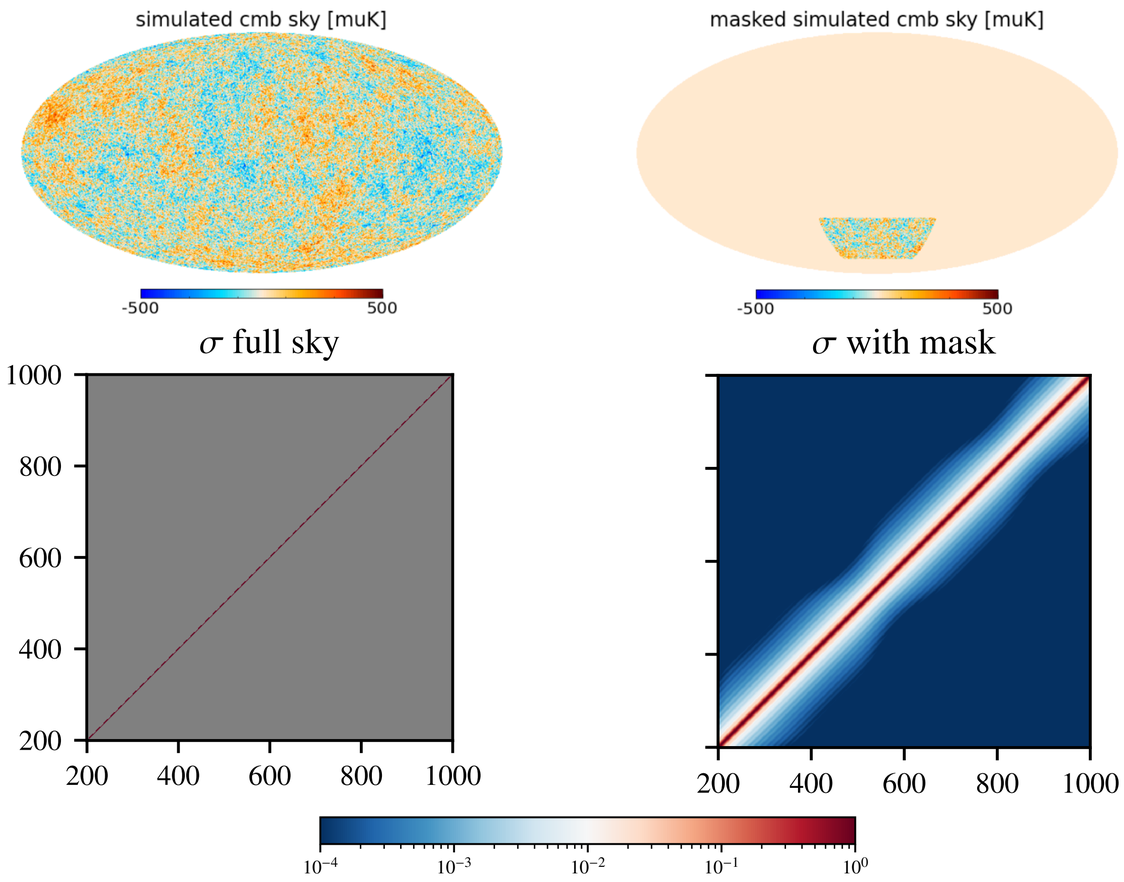

Pipeline improvements 2018 —> 2019-2020

- Flat sky —> curved sky
- Covariance matrix from simulations —> Fast and accurate analytical computation of the covariance **[EC et al. 2022]**

- Precise
- Modular
- Corrected for instrumental effects and statistical anisotropies due to filtering

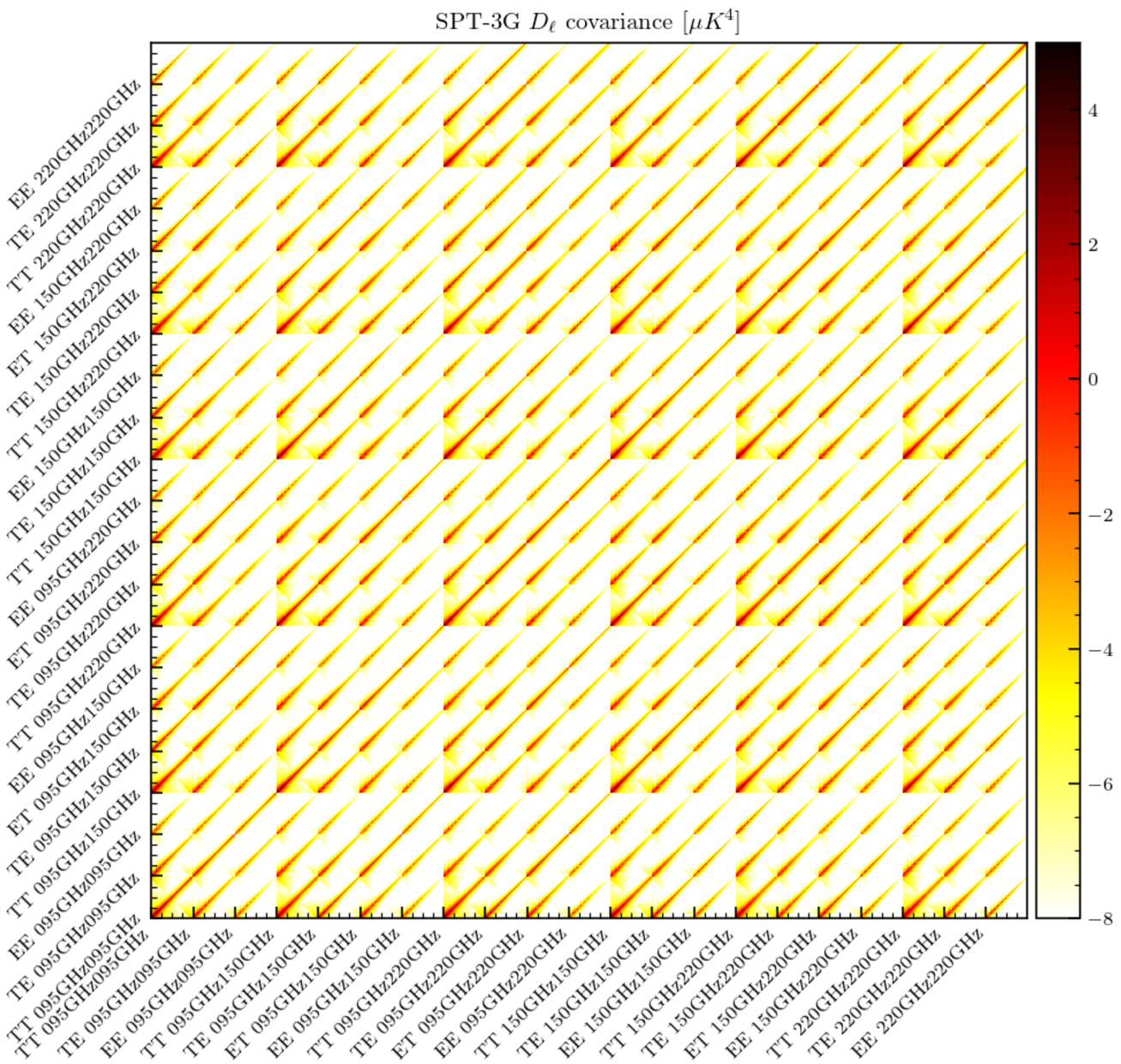

Pipeline improvements 2018 —> 2019-2020

- Flat sky —> curved sky
- Covariance matrix from simulations —> Fast and accurate analytical computation of the covariance **[EC et al. 2022]**
- ~170 sources masked —> ~2500 sources masked
  2118 radio sources with flux > 6mJy
  537 clusters with SNR > 10

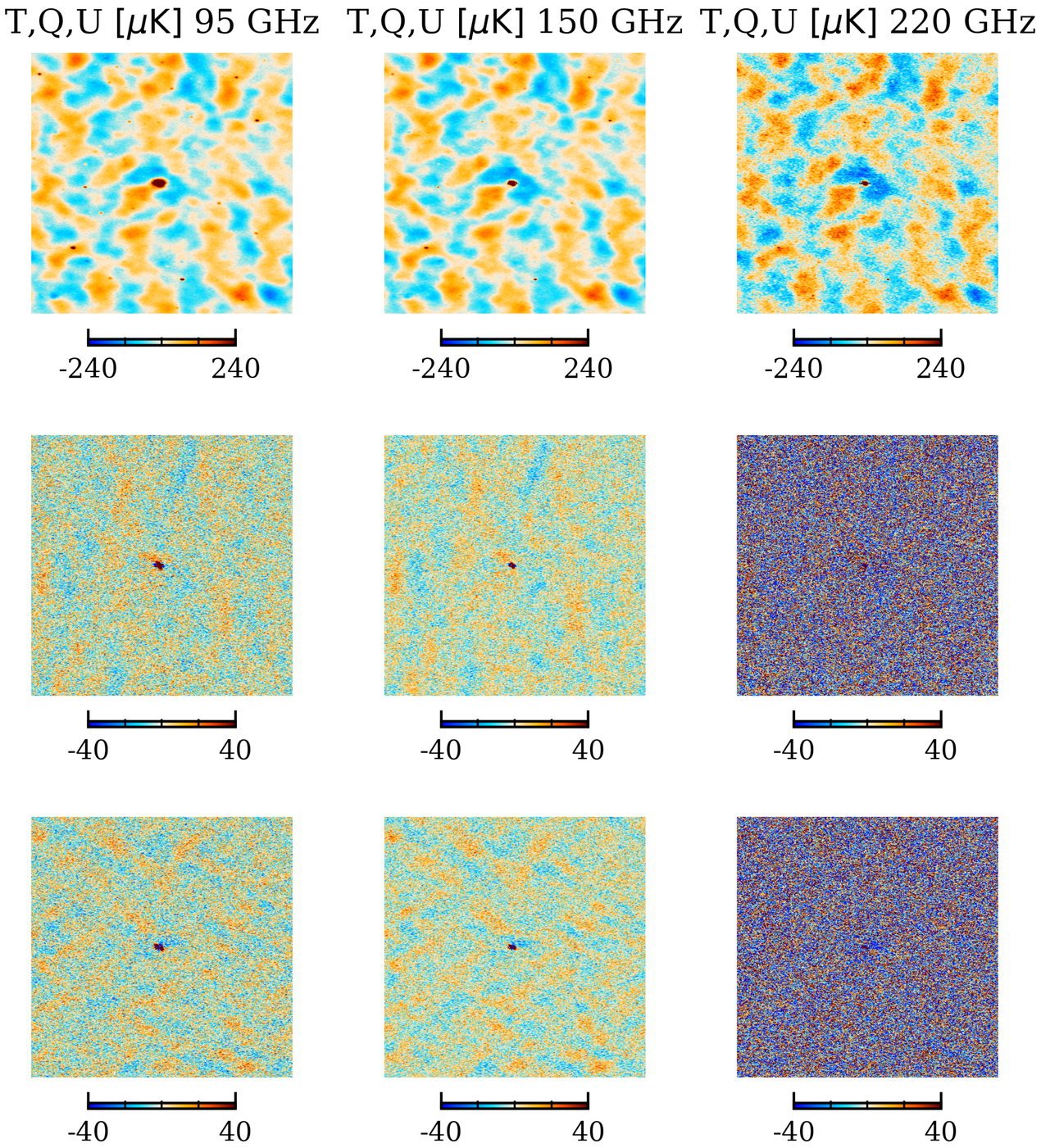

Pipeline improvements 2018 —> 2019-2020

- Flat sky —> curved sky
- Covariance matrix from simulations —> Fast and accurate analytical computation of the covariance **[EC et al. 2022]**
- ~170 sources masked —> ~2500 sources masked
  2118 radio sources with flux > 6mJy
  537 clusters with SNR > 10

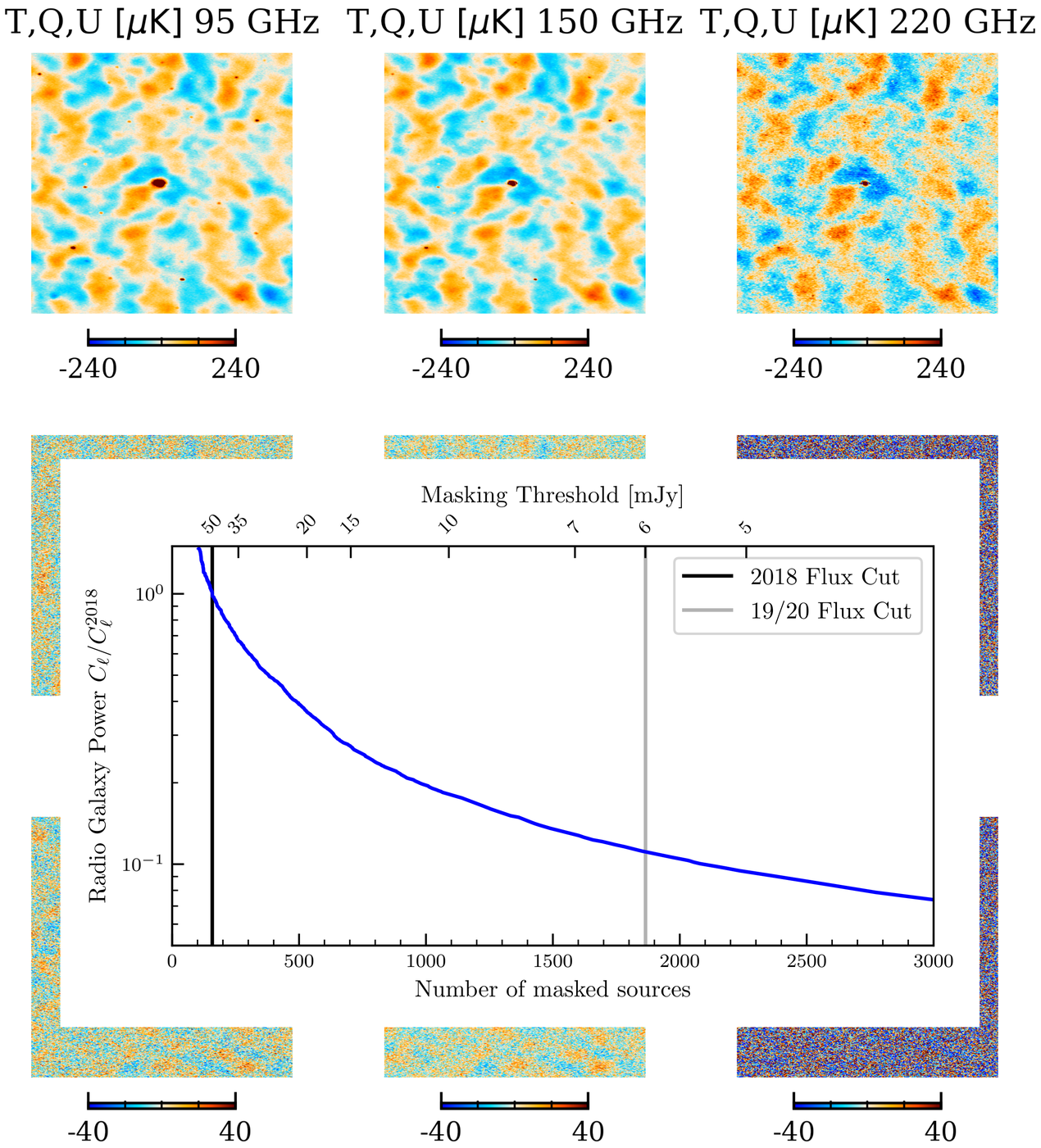

Pipeline improvements 2018 —> 2019-2020

- Flat sky —> curved sky
- Covariance matrix from simulations —> Fast and accurate analytical computation of the covariance **[EC et al. 2022]**
- ~170 sources masked —> ~2500 sources masked
  2118 radio sources with flux > 6mJy
  537 clusters with SNR > 10

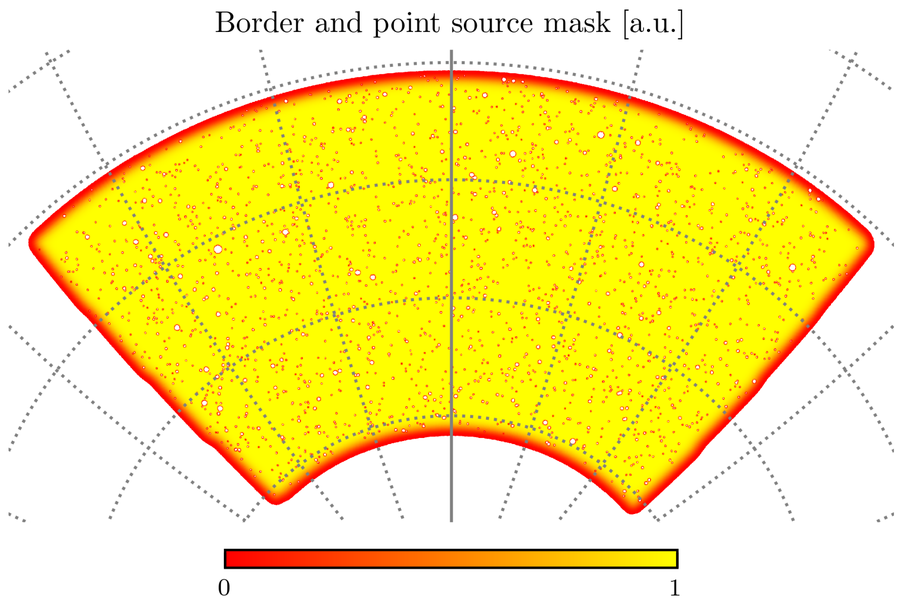

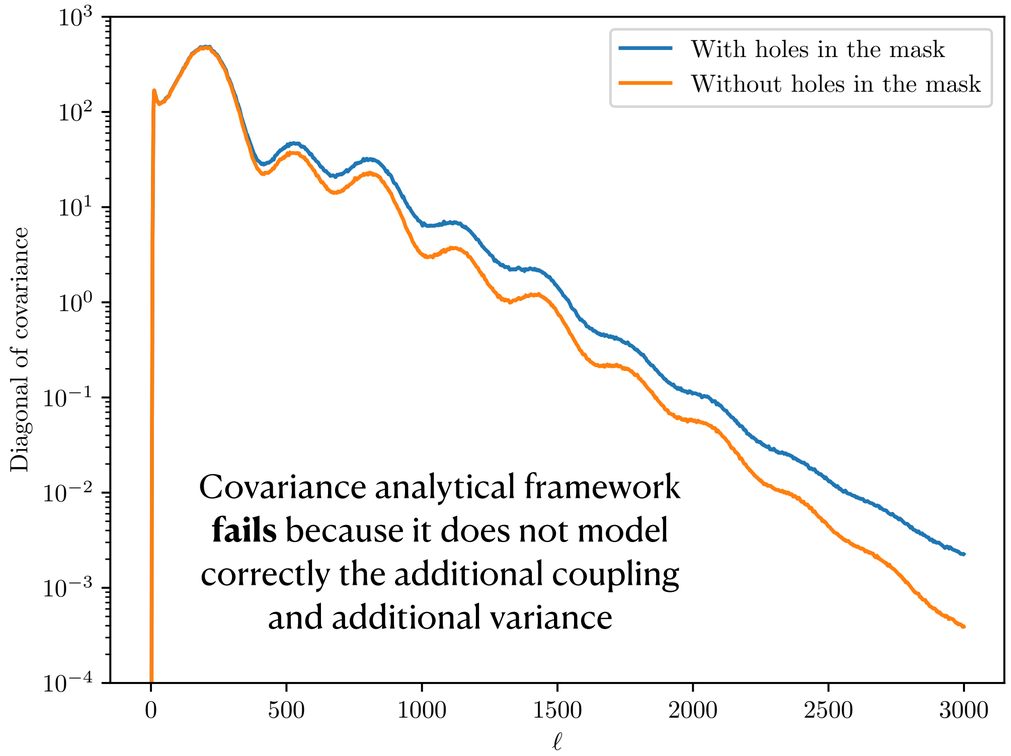

Pipeline improvements 2018 —> 2019-2020

- Flat sky —> curved sky
- Covariance matrix from simulations —> Fast and accurate analytical computation of the covariance **[EC et al. 2022]**
- ~2500 sources are masked in the field **High precision Gaussian constrained realization of the CMB anisotropies [EC, Benabed et al., *in prep*]**

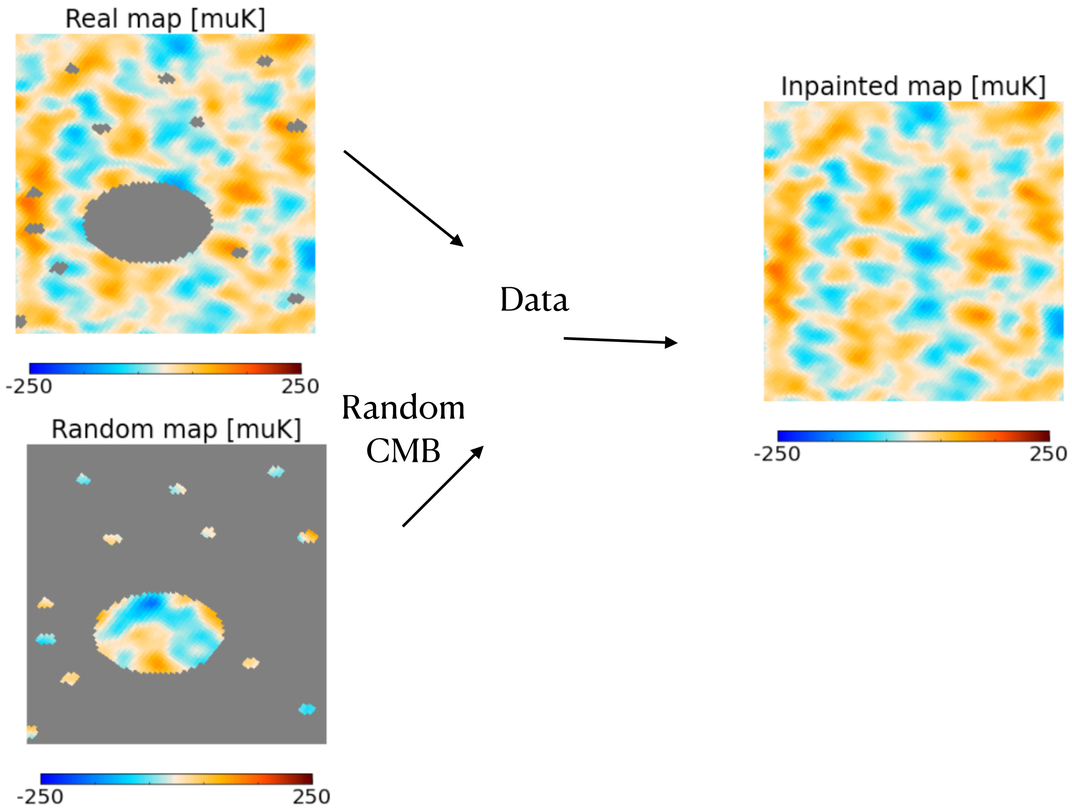

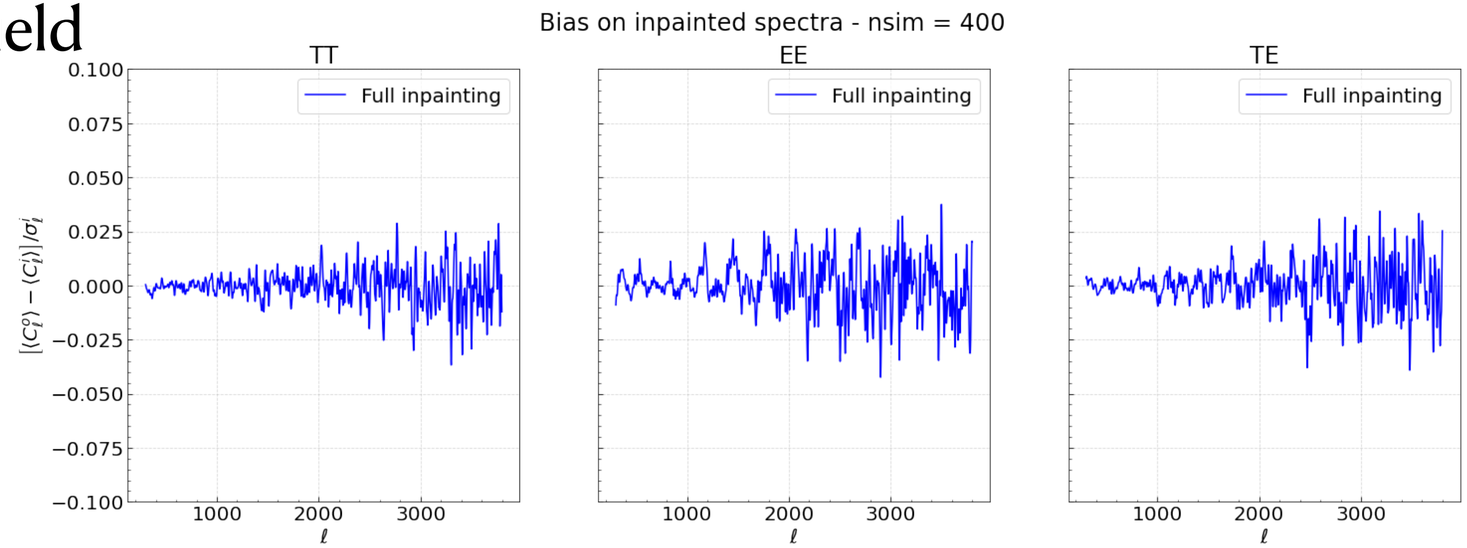

Perspectives

- Finalize null tests
- Ongoing likelihood implementation in JAX (differentiability)
- Run **consistency checks**
- Speed up MCMC chains as for SPT-3G 2018 with CosmoPower (Spurio Mancini et al. 2022)
- **Blinded analysis**
- Results coming soon !

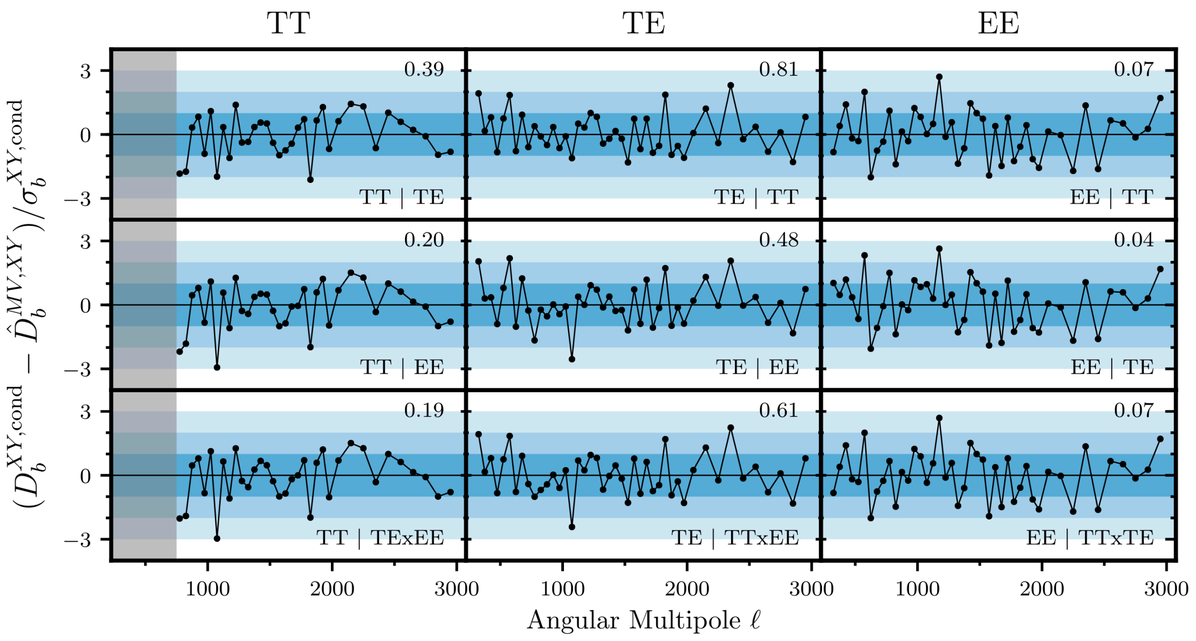

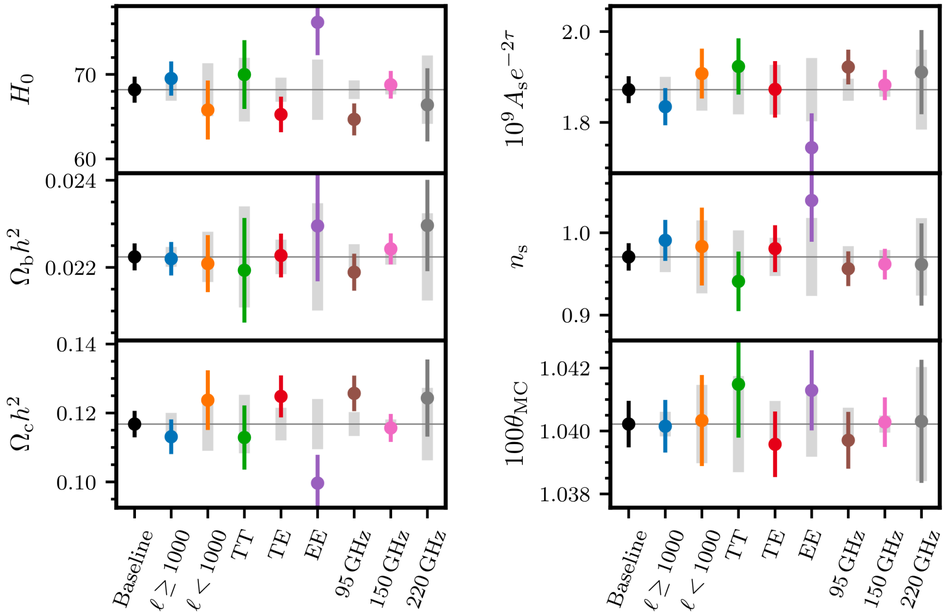

Credits: Aman Chokshi

Conclusions

SPT-3G 19/20 will put tight constraints on parameters

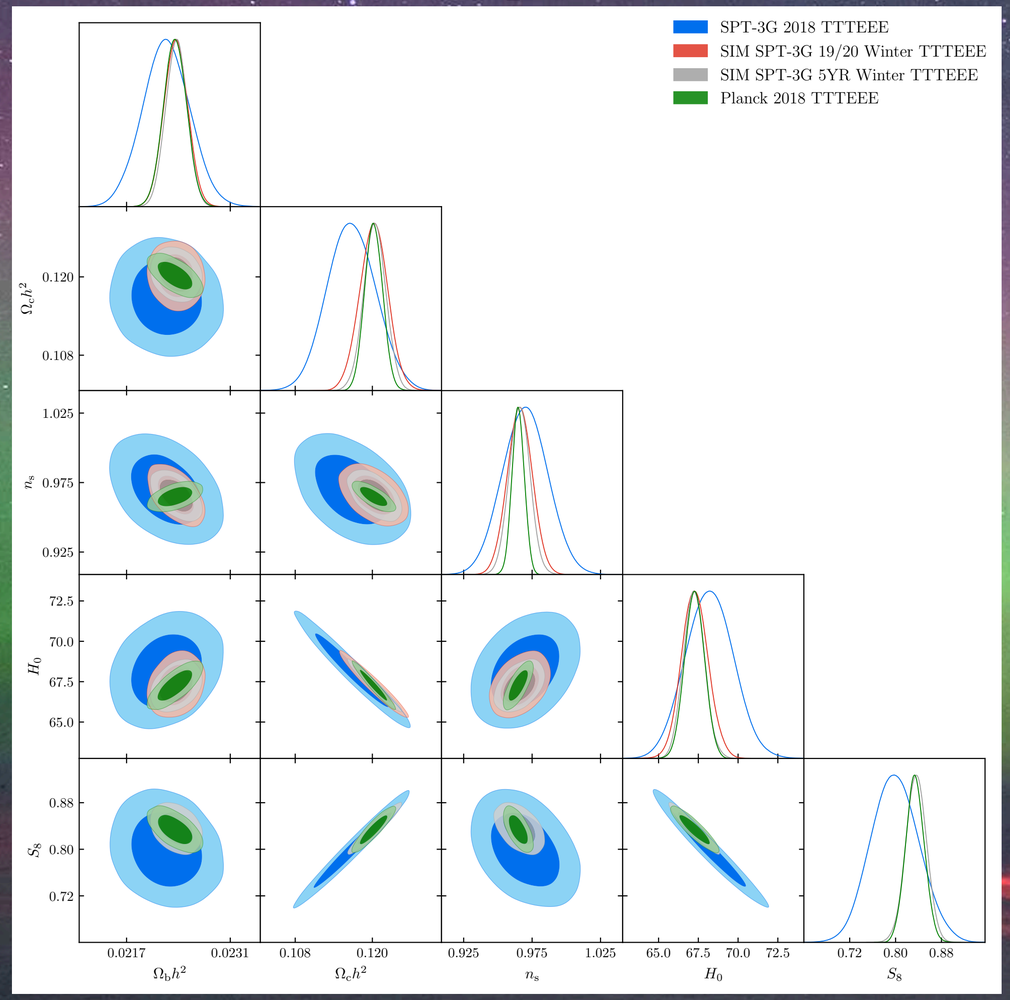

Significant improvements to the pipeline

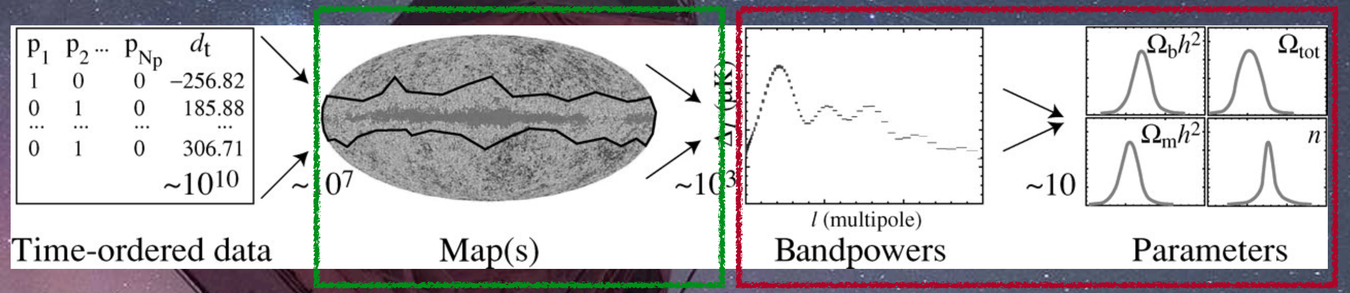

High-precision CMB inpainting

[EC, Benabed, *in prep*]

Accurate CMB covariance matrices

[EC et al. 2022]

n_s Ω_b degeneracy in ACT results

from Aiola et al. 2020

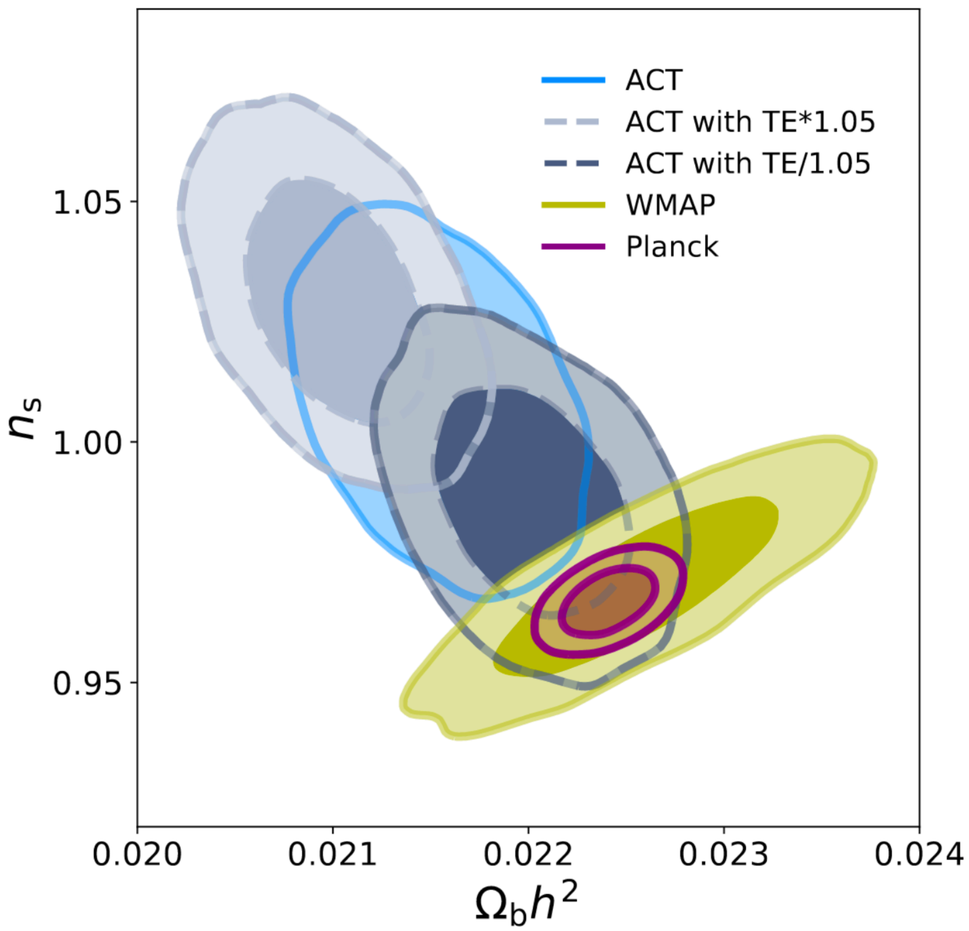

Noise levels and beams

Frequency	SPT-3G FWHM [′]	*Planck* FWHM [′]	ACT FWHM [′]
95GHz	1.57	9.7	2.0
150GHz	1.17	7.2	1.3 to 1.46
220GHz	1.04	5.0	NA

Frequency	SPT-3G 19/20		SPT-3G 2018		*Planck*		ACT DR4	
	TT	EE	TT	EE	TT	EE	TT deep	TT wide (AA)
95GHz	5.4	8.1	20.9	29.6	77.4	118	> 18.4	72.9
150GHz	4.6	6.6	14.9	21.1	33	70	> 12.6	118.5
220GHz	16	23	53	75	46.8	105	NA	NA

Foregrounds

From SPT-3G 2018 - Balkenhol et al. 2022

Temperature		
$A_{80}^{\rm cirrus}$	$\mathcal{N}(1.88, 0.48)$ [1.93]	Galactic cirrus amplitude
$\alpha^{\rm cirrus}$	$\mathcal{N}(-2.53, 0.05)$ [-2.53]	Galactic cirrus power law index
$\beta^{\rm cirrus}$	$\mathcal{N}(1.48, 0.02)$ [1.48]	Galactic cirrus spectral index
$D_{3000,95\times95}^{\rm Poisson,TT}$	$\mathcal{N}(51.3, 9.4)$ [62.61]	TT Poisson power for 95×95 GHz
$D_{3000,95\times150}^{\rm Poisson,TT}$	$\mathcal{N}(22.4, 7.1)$ [27.9]	TT Poisson power for 95×150 GHz
$D_{3000,95\times220}^{\rm Poisson,TT}$	$\mathcal{N}(20.7, 5.9)$ [24.3]	TT Poisson power for 95×220 GHz
$D_{3000,150\times150}^{\rm Poisson,TT}$	$\mathcal{N}(15.3, 4.1)$ [16.7]	TT Poisson power for 150×150 GHz
$D_{3000,150\times220}^{\rm Poisson,TT}$	$\mathcal{N}(28.4, 4.2)$ [28.6]	TT Poisson power for 150×220 GHz
$D_{3000,220\times220}^{\rm Poisson,TT}$	$\mathcal{N}(76.0, 14.9)$ [78.5]	TT Poisson power for 220×220 GHz
$A_{80}^{\rm CIB-cl.}$	$\mathcal{N}(3.2, 1.8)$ [5.2]	CIB clustering amplitude
$\beta^{\rm CIB-cl.}$	$\mathcal{N}(2.26, 0.38)$ [1.85]	CIB clustering spectral index
$A^{\rm tSZ}$	$\mathcal{N}(3.2, 2.4)$ [4.7]	tSZ amplitude
ξ	$\mathcal{N}(0.18, 0.33)$ [0.09]	tSZ-CIB correlation
$A^{\rm kSZ}$	$\mathcal{N}(3.7, 4.6)$ [3.7]	kSZ amplitude
Polarization		
$D_{3000,95\times95}^{\rm Poisson,EE}$	$\mathcal{N}(0.041, 0.012)$ [0.041]	EE Poisson power for 95×95 GHz
$D_{3000,95\times150}^{\rm Poisson,EE}$	$\mathcal{N}(0.0180, 0.0054)$ [0.0177]	EE Poisson power for 95×150 GHz
$D_{3000,95\times220}^{\rm Poisson,EE}$	$\mathcal{N}(0.0157, 0.0047)$ [0.0157]	EE Poisson power for 95×220 GHz
$D_{3000,150\times150}^{\rm Poisson,EE}$	$\mathcal{N}(0.0115, 0.0034)$ [0.0115]	EE Poisson power for 150×150 GHz
$D_{3000,150\times220}^{\rm Poisson,EE}$	$\mathcal{N}(0.0190, 0.0057)$ [0.0188]	EE Poisson power for 150×220 GHz
$D_{3000,220\times220}^{\rm Poisson,EE}$	$\mathcal{N}(0.048, 0.014)$ [0.048]	EE Poisson power for 220×220 GHz
A_{80}^{TE}	$\mathcal{N}(0.120, 0.051)$ [0.138]	TE amplitude of polarized galactic dust
α_{TE}	$\mathcal{N}(-2.42, 0.04)$ [-2.42]	TE power law index of polarized galactic dust
β_{TE}	$\mathcal{N}(1.51, 0.04)$ [1.51]	TE spectral index of polarized galactic dust
A_{80}^{EE}	$\mathcal{N}(0.05, 0.022)$ [0.052]	EE amplitude of polarized galactic dust
α_{EE}	$\mathcal{N}(-2.42, 0.04)$ [-2.42]	EE power law index of polarized galactic dust
β_{EE}	$\mathcal{N}(1.51, 0.04)$ [1.51]	EE spectral index of polarized galactic dust

Analytical covariance matrices for small footprints

[EC et al. 2022]

1. Implement the first exact covariance code with a speed-up $\mathcal{O}(\ell_{\max}^5)$
2. List existing analytical approximations of covariance and propose a new one
3. Assert their precision against the exact code

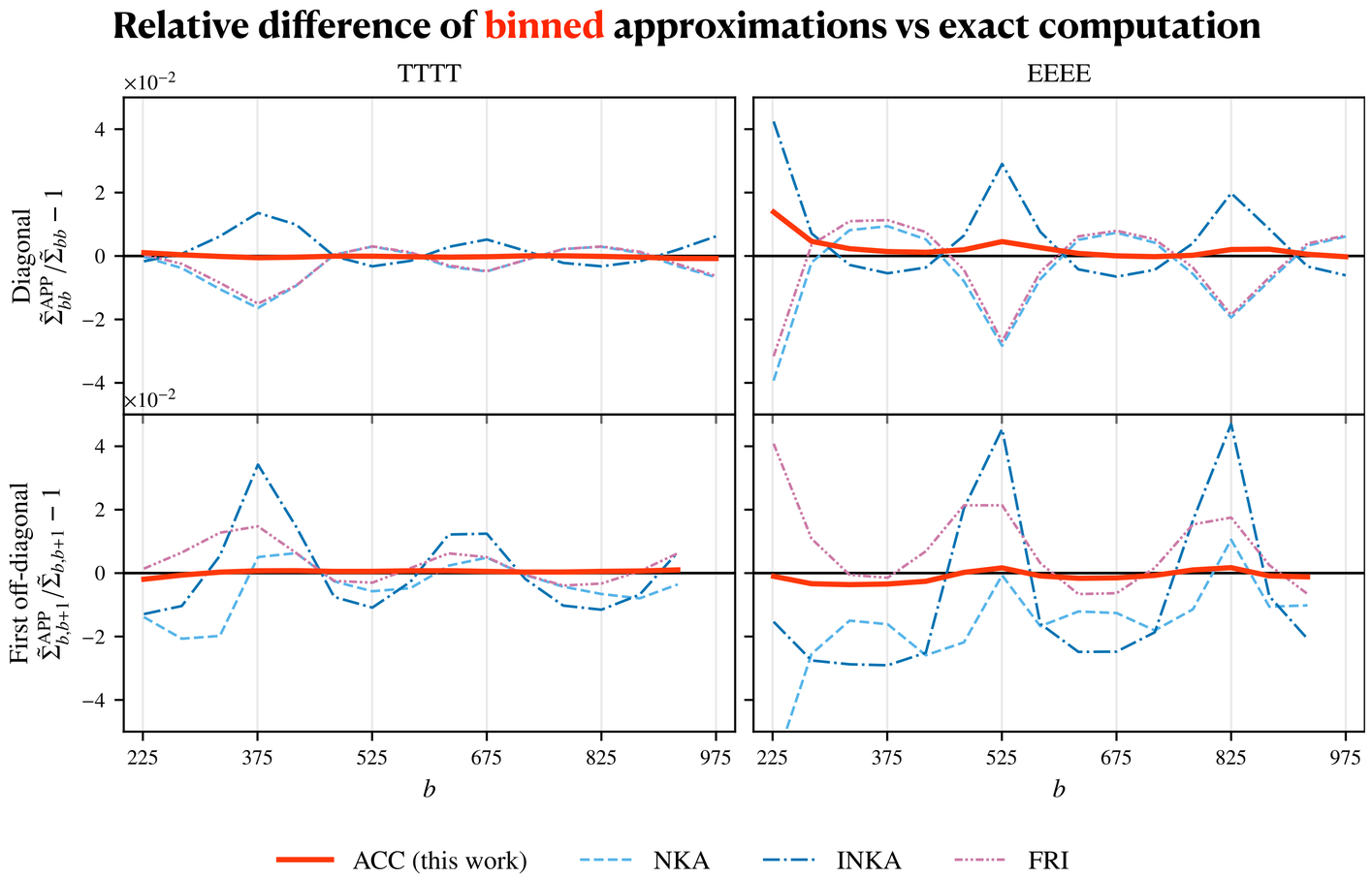

SPT-3G covariance

Applying our semi-analytical framework

1. SPT-3G maps are **anisotropically filtering**. The analytical framework should fail
2. We **adapted the analytical covariance framework** to take into account those anisotropies, using a 1D correction [Hivon, Doussot et al. in prep]
   Plot: ratio of diagonals analytical framework over simulations

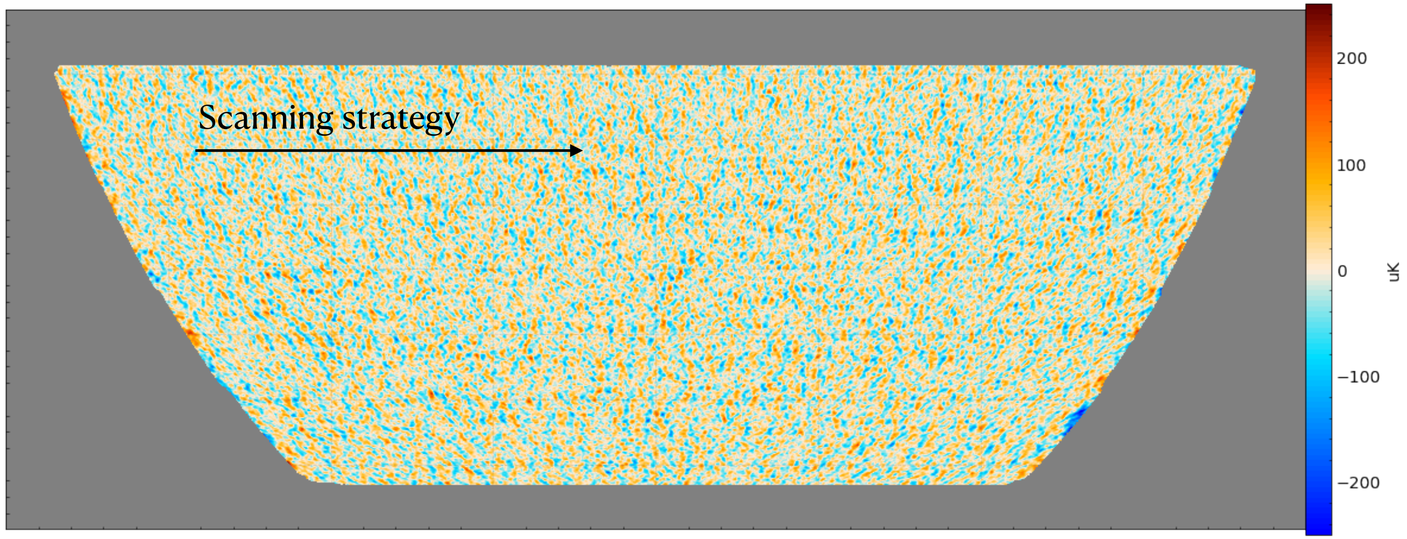

CMB temperature map with anisotropic filter

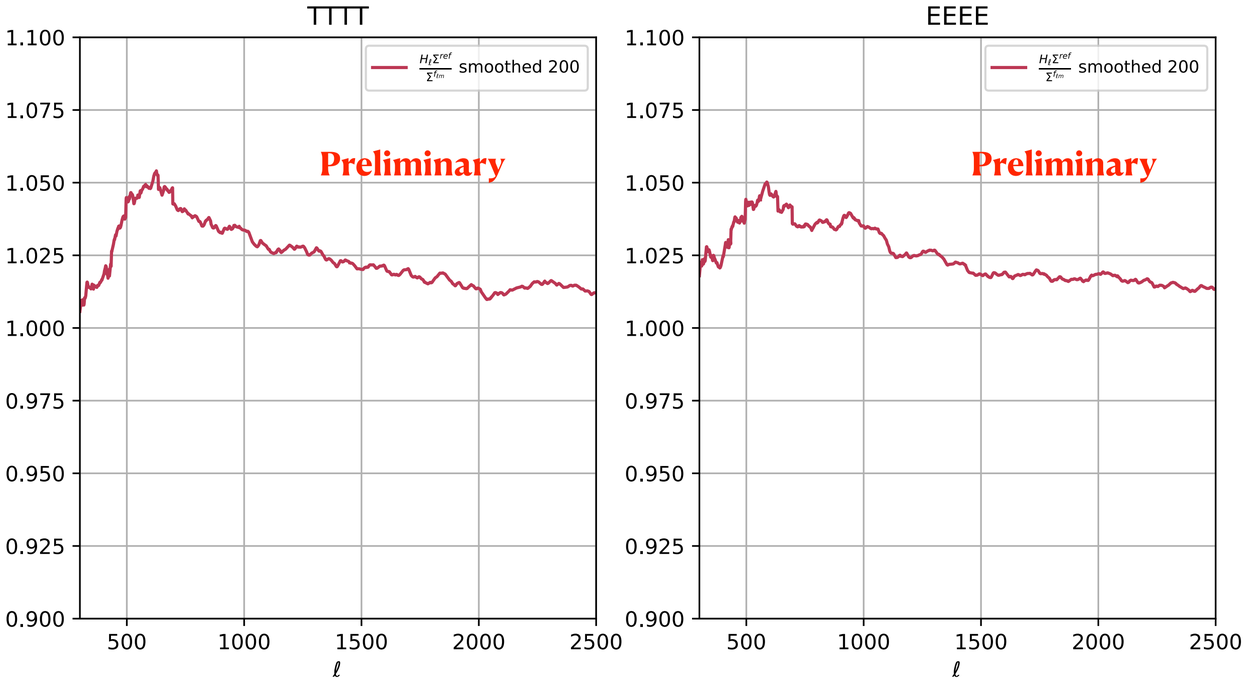

Ratio of diagonals : (Analytical covariance)/(Simulations with 2D filtering)

More about tensions

Results on tensions

Hubble constant

H_0 = 68.3 ± 1.5 km s^{-1} Mpc^{-1} (SPT3G 2018 TTTEEE)

Consistent with Planck (H_0 = 67.36 ± 0.54 km s^{-1} Mpc^{-1})
2.8σ lower than Sh0es value Murakami+ 2023
(H_0 = 73.29 ± 0.9 km s^{-1} Mpc^{-1})

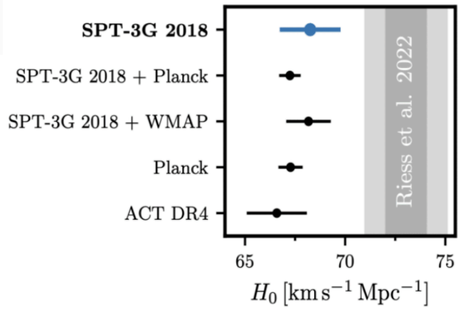

Growth of structure

S_8 = 0.797 ± 0.042

Consistent with Planck (S_8 = 0.832 ± 0.013)
Consistent with weak lensing measurements e.g KiDS+DES ($0.790^{+0.018}_{-0.014}$)

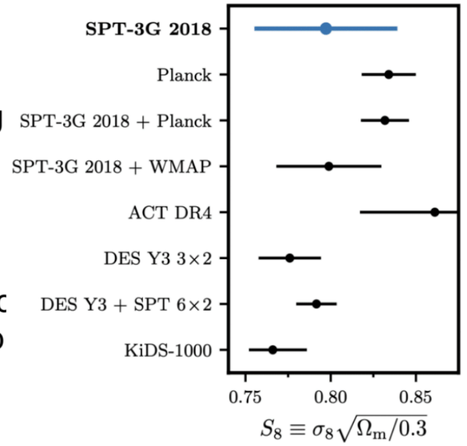

Lensing amplitude (LCDM+Alens)

A_L = 0.87 ± 0.11 consistent with unity, contrary tc Planck which gives a 2-3 sigma excess (but erro are twice larger for SPT).

No deviations from LCDM

credits Silvia Galli

Foregrounds

From SPT-3G 2018 - Balkenhol et al. 2022

$$
\begin{cases}
D^{\mathrm{cirrus}}_{\ell,\nu\times\mu} = A^{\mathrm{cirrus}}_{80}\dfrac{g(\mu)g(\nu)}{g(\nu_0^{\mathrm{cirrus}})^2}\left(\dfrac{\nu\mu}{(\nu_0^{\mathrm{cirrus}})^2}\right)^{\beta^{\mathrm{cirrus}}}\left(\dfrac{\ell}{80}\right)^{\alpha^{\mathrm{cirrus}}+2} \quad \text{with varying } \left[A^{\mathrm{cirrus}}_{80}, \beta^{\mathrm{cirrus}}, \alpha^{\mathrm{cirrus}}\right], \\
D^{\mathrm{TT,Poisson}}_{\ell,\nu\times\mu} = D^{\mathrm{TT,Poisson}}_{3000,\nu\times\mu}\left(\dfrac{\ell}{3000}\right)^2 \quad \text{with varying } \left[D^{\mathrm{TT,Poisson}}_{3000,\nu\times\mu},\ \forall\nu,\mu\right], \\
D^{\mathrm{CIB-cl.}}_{\ell,\nu\times\mu} = A^{\mathrm{CIB-cl.}}_{80}\dfrac{g(\mu)g(\nu)}{g(\nu_0^{\mathrm{CIB-cl.}})^2}\left(\dfrac{\nu\mu}{(\nu_0^{\mathrm{CIB-cl.}})^2}\right)^{\beta^{\mathrm{CIB-cl.}}}\left(\dfrac{\ell}{80}\right)^{0.8} \quad \text{with varying } \left[A^{\mathrm{CIB-cl.}}_{80}, \beta^{\mathrm{CIB-cl.}}\right], \\
D^{\mathrm{tSZ}}_{\ell,\nu\times\mu} = A^{\mathrm{tSZ}}\dfrac{f(\nu)f(\mu)}{f(\nu_0^{\mathrm{tSZ}})^2}D^{\mathrm{tSZ,template}}_{\ell} \quad \text{with varying } \left[A^{\mathrm{tSZ}}\right], \\
D^{\mathrm{tSZ-CIB}}_{\ell,\nu\times\mu} = -\xi\left(\sqrt{D^{\mathrm{tSZ}}_{\ell,\nu\times\nu}D^{\mathrm{CIB-cl.}}_{\ell,\nu\times\nu}} + \sqrt{D^{\mathrm{tSZ}}_{\ell,\mu\times\mu}D^{\mathrm{CIB-cl.}}_{\ell,\mu\times\mu}}\right) \quad \text{with varying } [\xi], \\
D^{\mathrm{kSZ}}_{\ell} = A^{\mathrm{kSZ}}D^{\mathrm{kSZ,template}}_{\ell} \quad \text{with varying } \left[A^{\mathrm{kSZ}}\right].
\end{cases}
$$

Reichardt et al. 2020

SPT-3G winter+summer footprints and Planck 30 GHz

Temperature

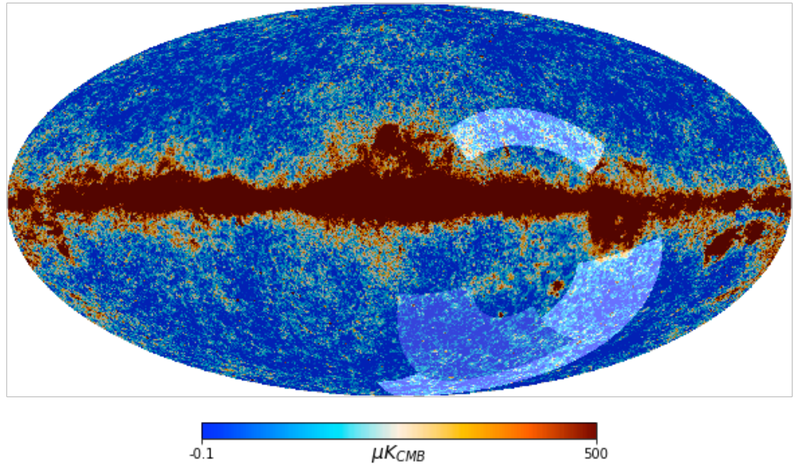

Polarization

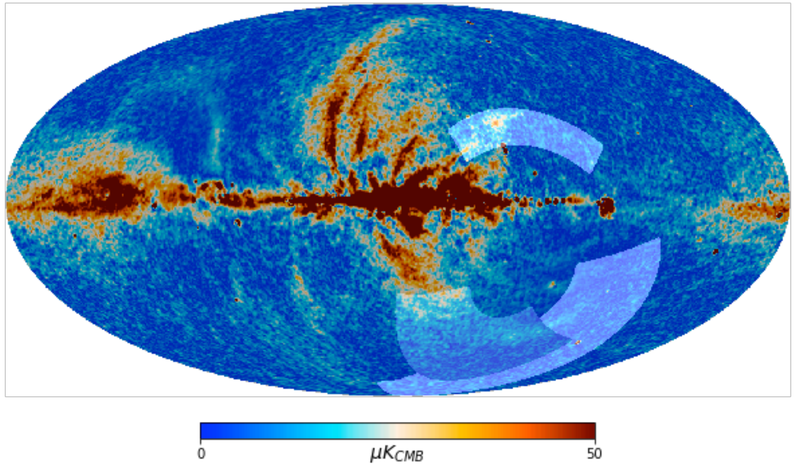

SPT-3G winter+summer footprints and Planck 353 GHz